

Collisional diffusion of a partially-ionized plasma in a magnetic field

A. P. Zhilinskii and L. D. Tsendin

M. I. Kalinin Polytechnic Institute, Leningrad
Usp. Fiz. Nauk **131**, 343–385 (July 1980)

The principal mechanisms of classical diffusion (due to binary collisions) of a partially-ionized plasma in a homogeneous magnetic field are examined. As a result of anisotropy of the transport coefficients of charged particles the problem proves to be far more complicated than the well-known problem of ambipolar diffusion in the absence of a magnetic field. The evolution of diffusion in this case is determined primarily by eddy currents flowing in the plasma. The circuit for these currents can be completed both through the background plasma giving rise to depletion regions, and by the conducting walls of the container of the plasma (the short-circuit effect). Ambipolar diffusion which occurs when the electron and ion fluxes are equal at every point can be realized only in exceptional cases. Experiments are described in which the short-circuit effect and ambipolar diffusion were observed. Using different boundary conditions it was possible to vary the diffusion rate of the plasma by two or three orders of magnitude, and this presents the possibility of controlling the local parameters of the plasma. This review has taken into account references up to July, 1979.

PACS numbers: 52.25.Fi

CONTENTS

1. Introduction	331
2. Initial equations. Unipolar diffusion	332
3. Evolution of concepts concerning the effect of a self-consistent electric field on diffusion	333
4. Diffusion in the absence of a magnetic field	336
5. Spreading of a density perturbation in an infinite plasma in a magnetic field	337
a. Small perturbations without an external current	337
b. Evolution of a nonlinear perturbation	340
c. Allowance for an external current	341
d. Spreading of a plasma pinch	342
e. Experiments in the ionospheric plasma	343
6. Diffusion of plasma in a finite volume	344
a. Effective boundary conditions	344
b. Diffusion in a dielectric apparatus	344
c. Diffusion in an apparatus with conducting walls	347
d. Diffusion in the case of more complex boundary conditions	349
e. Diffusion probe in a magnetic field	351
References	353

1. INTRODUCTION

Diffusion of charged particles in a quasistationary magnetic field constitutes one of the principal problems of contemporary plasma physics. In this review, we shall confine our analysis to diffusion of a weakly-ionized plasma in which the charged particle pressure is considerably lower than the neutral gas pressure and the magnetic pressure $H^2/8\pi$. Moreover, we shall consider the magnetic field and the neutral gas density to be uniform and stationary. The range of practical problems which are associated with the diffusion effects under consideration is very wide. Within this range we should include a number of problems of gaseous¹⁻⁶ and semiconductor⁷⁻⁹ electronics, MHD energy conversion,^{3,10} ionospheric physics,¹¹⁻¹³ etc. Similar processes take place in the near-wall regions of hot-plasma devices for controlled thermonuclear fusion.

In recent years, significant advances have been made in constructing a general model of evolution of a non-

uniform weakly-ionized plasma in a magnetic field. Progress in this area is connected primarily with being able to separate, in a number of experiments, effects associated with plasma turbulence from phenomena to which boundaries and collisional transport in the volume give rise. On the other hand, the simplest problems were subjected to systematic theoretical analysis. Thus, an unambiguous comparison of the collisional (classical) and turbulent diffusion theory with experiment was made possible.

In this review, the simplest examples are used to analyze the basic mechanisms which determine the evolution of plasma inhomogeneities in a magnetic field and the diffusion of a confined plasma to the walls. It turns out that the diffusion processes in a magnetic field are determined primarily by the flow of eddy currents which are produced by a self-consistent electric field. Thus, for example, ambipolar diffusion, characterized by equal electron and ion currents at each point and by the absence of eddy currents, may take place only in

relatively rare cases.

The fundamental physical concepts described below are based only on the difference between and the anisotropy of the diffusion coefficients and the mobilities of electrons and ions. Thus, similar effects should occur in a turbulent plasma (at least as long as the particle motion is confined to small random wandering) and in those semiconductors in which the transport coefficients may exhibit anisotropy, even in the absence of a magnetic field. However, we shall practically disregard problems associated with a quantitative analysis of charged particle diffusion under these conditions. We shall merely note that in the case of a turbulent plasma the values of the anomalous transport coefficients are determined by turbulence characteristics (see, e.g., Refs. 14-18), while the nature of instability and of the turbulence, which instability produces as it develops, depends to a large degree on the properties of the equilibrium state. Thus, analysis of the latter constitutes, in fact, the first step toward a solution of the anomalous transport problem under real conditions.

2. INITIAL EQUATIONS. UNIPOLAR DIFFUSION

We shall state the diffusion equations for the simplest case of a weakly-ionized plasma with singly-charged ions of one kind [we shall call this three-component plasma, consisting of electrons (e), ions (i) and atoms (a), "simple"]. If collisions between the charged particles are unimportant (a weakly-ionized plasma), the following equations describe diffusion in a system of coordinates associated with the neutral gas:

$$\frac{\partial n_\alpha}{\partial t} + \nabla \Gamma_\alpha = I_\alpha, \quad (1)$$

$$\Gamma_\alpha = n_\alpha \mathbf{u}_\alpha = -\hat{D}_\alpha \nabla n_\alpha \pm n_\alpha \hat{b}_\alpha E, \quad (2)$$

$$\nabla E = 4\pi e (n_i - n_e); \quad (3)$$

where the index α corresponds to ions (i) or electrons (e), Γ_α are particle fluxes and I_α are terms describing the production and recombination of charged particles, which are neglected in all cases under consideration in this review. The motion of the neutral gas may be considered as given. Questions associated with the inverse effect of plasma motion on the neutral gas are considered, for example, in Refs. 11, 19 and 20. If the particle energy distribution is Maxwellian, the unipolar mobility and diffusion tensors \hat{b}_α and \hat{D}_α , respectively, are related by the Einstein relations

$$\hat{D}_\alpha = \frac{\hat{b}_\alpha T_\alpha}{e}. \quad (4)$$

For the sake of simplicity, we shall limit further considerations to this case. The values of transport coefficients, which are determined by binary particle collisions, are conventionally referred to as classical. Their form is simplest in the case where the transport collision frequencies of the charged and neutral particles ν_α are independent of speeds. Moreover, in a constant magnetic field along the z -axis we have

$$\left. \begin{aligned} D_{\alpha zz} &\equiv D_{\alpha \parallel} = \frac{T_\alpha}{m_\alpha \nu_\alpha}, \\ D_{\alpha xx} &= D_{\alpha yy} \equiv D_{\alpha \perp} = D_{\alpha \parallel} \left[1 + \left(\frac{\Omega_\alpha}{\nu_\alpha} \right)^2 \right]^{-1}, \\ D_{\alpha xy} &= -D_{\alpha yx} \equiv D_{\alpha d} = D_{\alpha \parallel} \frac{\Omega_\alpha}{\nu_\alpha} \left[1 + \left(\frac{\Omega_\alpha}{\nu_\alpha} \right)^2 \right]^{-1}. \end{aligned} \right\} \quad (5)$$

where $\Omega_\alpha = eH/cm_\alpha$ is the cyclotron frequency. In the general case, expressions for the components of the \hat{D}_α tensors include terms $\nu_\alpha(v)$, which are in various ways averaged with respect to the particle distribution. The values of \hat{D}_α and \hat{b}_α for different particle interaction modes, ionization degrees and magnetic field intensities are given in a large number of review articles and monographs (see, for example, Refs. 5, 20, 21). In the case of rough calculations, so-called elementary theory^{22,23} is frequently used, whereby the $\nu_\alpha(v)$ averaged over the Maxwellian distribution are used in Eq. (5); the error introduced by this procedure is, as a rule, small.²² Below, we shall also utilize the elementary theory.

The terms $D_{\alpha d}$ describe a diamagnetic current which is independent of the translation of the guiding centers of the Larmor orbits. Thus, the divergence of the corresponding currents is identically equal to zero. The nondiagonal mobility terms $b_{\alpha d}$ define the Hall currents which may lead to spatial redistribution of particles.

If the particle concentration is sufficiently small, such that the Debye radii ($r_D = \sqrt{T_\alpha/4\pi n_\alpha e^2}$) are much larger than the dimensions of the system, the self-consistent electric field is, according to the Poisson equation [Eq. (3)], unimportant. In this case, in the absence of an external electric field a unipolar (free) diffusion of charged particles takes place and can be described as follows:

$$\frac{\partial n_\alpha}{\partial t} = \nabla (\hat{D}_\alpha \nabla n_\alpha). \quad (6)$$

In other words, diffusion of particles simply occurs in an anisotropic medium. The unipolar electron and ion diffusion in the magnetic field was studied experimentally in a number of articles.²⁴⁻²⁷ These articles convincingly show that the process is fully determined by the binary collisions and is well described by Eqs. (5) and (6). Figure 1 shows a summary of the experimental data for the case of unipolar diffusion of electrons and ions in helium.

The classical diffusion of charged particles in a magnetic field is, therefore, strongly anisotropic. The reason for this is that the values of the longitudinal and transverse components of \hat{D}_α are determined by the step of the random walks. The step along the magnetic field equals the mean free path of the particles λ_α ; consequently, $D_{\alpha \parallel} \sim \lambda_\alpha^2 \nu_\alpha$ and $D_{e \parallel} \gg D_{i \parallel}$. In the case of a strong transverse magnetic field H where the Larmor radius ρ_α is smaller than λ_α , the step is ρ_α . In view of this, the transverse coefficients sharply decrease with the field growth ($\sim H^{-2}$) and when

$$\rho_\alpha \rho_l < \frac{\lambda_\alpha \lambda_l T_l}{T_e} \quad (7)$$

the transverse diffusion of electrons becomes smaller than that of the ions. Throughout our analysis below, we shall consider the magnetic field to be sufficiently strong to satisfy the inequality in Eq. (7).

In the case of infinite problems, it is convenient to introduce characteristic unipolar scales for the spreading of a disturbance along and across the mag-

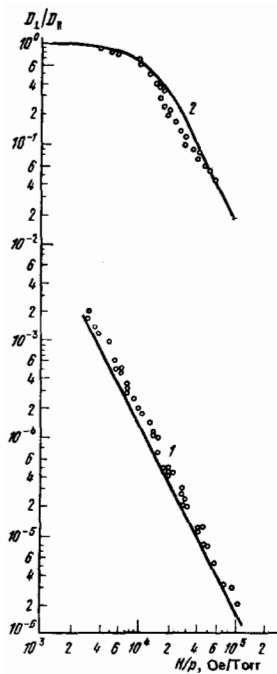


FIG. 1. Effect of magnetic field on the transverse diffusion of charged particles. 1—electrons,^{5,24,25} 2—ions,^{26,27} lines— theoretical calculations, circles—experiment.

netic field for particles of a given kind:

$$\Lambda_{\alpha\parallel}^2 = 4D D_{\alpha\parallel} t, \quad \Lambda_{\alpha\perp}^2 = 4D D_{\alpha\perp} t, \quad (8)$$

and for a plasma of finite dimensions ($\Lambda_{\parallel}, \Lambda_{\perp}$), it is convenient to introduce the characteristic lifetimes (diffusion to the walls):

$$\tau_{\alpha\parallel} = \frac{\Lambda_{\parallel}^2}{D_{\alpha\parallel}}, \quad \tau_{\alpha\perp} = \frac{\Lambda_{\perp}^2}{D_{\alpha\perp}}. \quad (9)$$

In the case where the condition (7) holds we have

$$\left(\frac{\Lambda_{\parallel e}}{\Lambda_{\parallel}}\right)^2 \sim \frac{T_e m_i v_i}{T_i m_e v_e} \gg 1, \quad \left(\frac{\Lambda_{\perp e}}{\Lambda_{\perp}}\right)^2 \sim \frac{T_e m_e v_e}{T_i m_i v_i} \left(1 + \frac{\rho_i^2}{\lambda_D^2}\right) \ll 1; \quad (10)$$

$$\frac{\Lambda_{\parallel e}}{\Lambda_{\perp e}} \sim \frac{\lambda_D}{v_e} \gg 1,$$

and, correspondingly

$$\tau_{e\parallel} \ll \tau_{i\parallel}, \quad \tau_{e\perp} \ll \tau_{i\perp}. \quad (11)$$

As the degree of ionization increases, the transport coefficients begin to experience the effect of charged particle collisions. If the particle energy is ≤ 10 eV, the Coulomb cross sections normally exceed the gas-kinetic cross sections severalfold, and these processes must already be taken into account at comparatively low degrees of plasma ionization. In the case $\nu_{ei} \ll (m_i/m_e)\nu_i$, the ion coefficients are determined, as before, by Eqs. (4) and (5), while for the electrons when $\Omega_e \gg \nu_e + \nu_{ei}$, $n_e = n_i$, we have, for example,

$$b_{e\perp} \approx \frac{mc^2}{eH^2} \left[v_0 + \frac{v_{ei}}{1 + (\Omega_e^2/\nu_e^2)} \right], \quad (12)$$

$$D_{e\perp} \approx \frac{mc^2}{e^2 H^2} T_e \left[\nu_e + \nu_{ei} \left(1 + \frac{T_i}{T_e} \frac{\Omega_e^2}{\Omega_i^2 + \nu_i^2} \right) \right]. \quad (13)$$

The values of the partial temperatures T_e and T_i should be determined, in principle, self-consistently through the corresponding energy balance equations. In this case, the thermal diffusion and conduction may be substantial and on a par with the field and diffusion cur-

rents. The flow of diffusion currents may itself lead to the occurrence of inhomogeneous partial temperature due to the diffusion thermoeffect and diffusion cooling.²⁸⁻³⁰ The resultant complex and diverse effects have been inadequately studied. We shall not be concerned with these problems and we shall assume that the particle temperatures are independent of the coordinates and time.

3. EVOLUTION OF CONCEPTS CONCERNING THE EFFECT OF A SELF-CONSISTENT ELECTRIC FIELD ON DIFFUSION

When the Debye radii become smaller than the dimensions of an inhomogeneity (apparatus), the nature of charged particle motion is essentially altered. This is due to the occurrence in a plasma of a self-consistent field which exhibits strong and, frequently, determining effect on the particle mobility. Actually, as the result of differences in the diffusion and drift rates, the electron and ion components of an inhomogeneity always tend to separate. However, even small decomposition of charges leads to the formation of an electric field which tends further to inhibit the separation of components. As a result of this, an inhomogeneity continues to move and spreads in such a manner that its electron and ion densities are almost identical and a quasineutrality is achieved.

The evolution of an arbitrary initial distribution with $n_e \neq n_i$ occurs, in this case, in two stages. At first, a quasineutral state is rapidly established. If the collisions occur sufficiently frequently so that the Maxwellian times $\tau_M(\mathbf{k}) = [4\pi\sigma(\mathbf{k})]^{-1}$ [$\sigma(\mathbf{k})$ is the plasma conductivity in the appropriate direction] are greater than the intervals between collisions, this occurs during a time $\sim \tau_M$.²⁰ Conversely, the establishment of quasineutrality may be accompanied by oscillations. The quasineutral density profile, formed in some arbitrary way, constitutes the initial condition for a slower diffusion stage of the evolution. During the latter stage substantial disturbances of quasineutrality may take place only near the plasma confining surfaces. Since we are interested in the diffusion processes, we may assume $n_e = n_i$ for the plasma volume and neglect the Poisson equation. The electric field is defined by the quasineutrality condition

$$\nabla \cdot (\Gamma_e - \Gamma_i) = 0. \quad (14)$$

In other words, the electric field is adjusted so as to avoid substantial separation of charges.

Normally, the diffusion processes proceed relatively slowly and the field nearly always may be considered as potential. The solution of the problem concerning diffusion of a simple weakly-ionized plasma in the absence of a magnetic field was obtained by Schottky as early as 1924.³¹ Moreover, it became apparent that the quasineutrality condition leads to the diffusion being ambipolar, i.e., the electric field may be eliminated from the system [Eqs. (1) and (2)], having reduced the latter to the following equation:

$$\frac{\partial n}{\partial t} = D_{a\perp} \Delta n, \quad (15a)$$

where

$$D_{a\parallel} = \frac{D_{e\parallel}b_{\parallel} + D_{i\parallel}b_{e\parallel}}{b_{e\parallel} + b_{i\parallel}} \approx \left(1 + \frac{T_e}{T_i}\right) D_{i\parallel} \quad (15b)$$

is the coefficient of ambipolar diffusion. Moreover, the density profile is independent of the current which flows through the plasma, and Eqs. (15a) and (15b) may be obtained simply by equating $\Gamma_e = \Gamma_i$. The ambipolar diffusion is determined by the slowest particles (ions) so that

$$\tau_{a\parallel} \approx \tau_{i\parallel} \left(1 + \frac{T_e}{T_i}\right)^{-1}. \quad (15c)$$

The electric field effect is confined to the coefficient $1 + (T_e/T_i)$ in Eqs. (15b) and (15c). We should point out a certain discrepancy in the terminology. Several authors interpret ambipolar diffusion as a process which satisfies the quasineutrality condition [Eq. (14)]. We shall refer to diffusion being ambipolar only in the case where the currents satisfy the conditions $\Gamma_{i\parallel} - \Gamma_{e\parallel} = j_{\parallel}/e = \text{const}$ and $\Gamma_{i\perp} - \Gamma_{e\perp} = j_{\perp}/e = \text{const}$ (j is the density of the through current; at $j=0$, $\Gamma_{e\parallel,\perp} = \Gamma_{i\parallel,\perp}$).

In a magnetic field, the simplest one-dimensional problems are also reduced to the ambipolar diffusion equation.³²⁻³⁴ Thus, in the case of diffusion along H , formulas in Eq. (15) are applicable and, in the case of transverse diffusion we have

$$D_{a\perp} \approx \left(1 + \frac{T_i}{T_e}\right) D_{e\perp}, \quad \tau_{a\perp} \approx \tau_{e\perp} \left(1 + \frac{T_i}{T_e}\right)^{-1}, \quad (16)$$

since the less mobile particles in this case are electrons. The results obtained in this manner have been used as a basis for many attempts (see, e.g., Refs. 35-38) to reduce multidimensional problems to the linear equation of ambipolar diffusion in an anisotropic medium. Moreover, the ambipolar condition $\Gamma_{e\parallel,\perp} = \Gamma_{i\parallel,\perp}$ satisfies the quasineutrality condition [Eq. (14)] and permits the elimination of the electric field from the initial system of equations. However, it can be easily verified⁵ that, in the general case, a potential electric field which satisfies this condition cannot be set up. In other words, the electric field which retards the more mobile particles in all directions (electrons along H and ions across) and equalizes currents at each point, cannot be achieved in the general case. Moreover, eddy currents present in the plasma decisively affect the evolution of the plasma density profile. The equations which describe diffusion spreading of an inhomogeneity turn out to be nonlinear and can not be reduced to the normal equation for diffusion in an anisotropic medium; the process is considerably more complex. The flow of the total current through an inhomogeneity under these conditions leads to a number of new phenomena—the density perturbation may travel and become deformed breaking up into separate plasma bunches; smoothing of the concentration is much faster in this case than without the current.²⁰

The eddy currents may flow both entirely in the plasma^{20,39} and partially along the conducting surfaces which confine the plasma and serve to complete the circuit.⁴⁰ The mechanism of the nonambipolar diffusion—constrained by the eddy currents—was studied for the first time by Simon⁴⁰ using plasma diffusion in a conducting chamber as example. If the chamber length (along H) is not too large, electrons should quickly

drift toward its ends. The plasma will become positively charged with respect to the walls and the electric field shall leave ions drifting across H unimpeded. This, therefore, gives rise to an eddy current which is carried along H by electrons and across by ions, and the circuit which is completed by the chamber walls. This phenomenon was called the “short circuiting effect.” The plasma lifetime (τ_{sc}), moreover, sharply decreases compared to the ambipolar lifetime, and is of the order of the greater of the “fast” times $\tau_{e\parallel}$, $\tau_{i\perp}$. The difference between τ_a and τ_{sc} , as can be seen from Eqs. (10) and (11), may exceed three orders of magnitude.

However, attempts to obtain an unambiguous proof of existence of the effect have been heretofore unsuccessful. More or less strict analytical^{41,42} or numerical⁴³ solutions of the Simon problem have encountered serious mathematical difficulties. These were associated first with the formulation of the boundary conditions, since the plasma equations are inapplicable near the walls—where boundary conditions are imposed on the potential—and, second, with the nonlinearity of the system of equations [Eqs. (1) and (2)]. However, the experimental results were ambiguous and even contradictory. The simplest experiments to interpret were those conducted for an infinite plasma. But, as far as we know, such studies were never conducted under laboratory conditions. Nevertheless, in the experiments conducted in the ionosphere (for example, in bariated clouds), the behavior of “tagged” ions was normally recorded rather than the total plasma density. Difficulties presented by laboratory experiments with a confined plasma were associated above all with the numerous instabilities acting on the gas-discharge plasma in the magnetic field. The resultant turbulent state is characterized by plasma lifetimes which are much shorter than “classical” (those due to the binary collisions). In an unstable plasma it is difficult to distinguish unambiguously a rise in diffusion (in comparison with ambipolar diffusion) due to turbulence from a similar rise resulting from eddy currents. Based on certain experiments, the foregoing has led to an expression of doubt concerning the feasibility of realizing the short-circuiting effect.⁴⁴ On the other hand, Geissler had proposed that the anisotropic nononedimensional diffusion of plasma even in a dielectric container is not, in general, ambipolar.⁴⁵ Lastly, it was asserted in Refs. 41, 46 that in a late stage of evolution the transport mechanism in a volume is fully determined by boundary conditions so that the diffusion is necessarily ambipolar in a dielectric chamber with walls parallel to H (see Section 6), and in a metallic chamber the short-circuiting effect should take place (and was observed in Ref. 41).^{41,46}

Thus, it was urgently necessary to provide a direct experimental proof of the effect of eddy currents on diffusion. To distinguish this effect it was necessary to obtain a quiescent plasma. It seems that the latter was produced in a strong magnetic field for the first time in Q -machines.⁴⁷⁻⁴⁹ However, because of the structural features, heretofore only the one-dimensional diffusion across H has been investigated in Q machines.

The problem of separating the eddy current and turbulence effects on the diffusion was solved by Zhilinskiĭ and Kuteev,⁵⁰ who obtained a quiescent decaying plasma in a metallic container for a broad range of conditions. They showed that the application of a difference of potential between the end and side conducting walls may be used to vary the lifetime of a quiescent plasma by almost three orders of magnitude, in agreement with theoretical ideas, from a value corresponding to short-circuiting to a value which exceeds the ambipolar lifetime. The lifetime of an unstable plasma, in which the transverse diffusion was due to a turbulence, was also strongly affected by varying the boundary conditions. Zhilinskiĭ and other coworkers have studied the effect of instability on the diffusion, have established the conditions under which ambipolar diffusion takes place in a dielectric chamber and have investigated the effects of more complex boundary conditions.⁵¹⁻⁵³ An unambiguous experimental discrimination of the basic transport mechanisms provides a solid basis for developing the theoretical concepts of plasma diffusion in the most diverse systems.

A systematic theoretical approach to the problems of multidimensional diffusion in a magnetic field and an analysis of the eddy current effects were attempted for the first time in Refs. 20, 54, 55. The spreading of a small point inhomogeneity against the background of an infinite plasma was investigated. It was shown that the problem in principle does not reduce to the ambipolar case. In particular, the shape of the constant density surfaces, even in the absence of an external current, has nothing in common with the ellipsoids which characterize diffusion in an anisotropic medium. Numerical calculations showed that the size of a perturbed region is determined, more likely, by the highest diffusion coefficients than by the lowest coefficients in the corresponding directions, as in the case of the ambipolar mechanism. The presence of an external current radically changes the entire picture of the evolution and leads to the separation of an initial perturbation into several bunches which travel and spread according to a fairly complex law. The behavior of the perturbation is not Gaussian, as one would naturally expect for the diffusion problem, but follows a power law ($\sim t/r^5$ in the absence and $\sim t/r^4$ in the presence of a current).

The mechanism underlying the effect of eddy currents on the diffusion spreading of an inhomogeneity in an infinite plasma was shown to be essentially similar to the Simon effect.⁵⁶ The "probing" electrons and ions injected into an infinite plasma (in the absence of an external current) diffuse mainly along and across the magnetic field, respectively. Quasineutrality is preserved by the motion of the background plasma. The latter, because of its high conductivity, acts in a certain sense not unlike conducting walls. The background plasma electrons and ions also move mainly along and across the magnetic field, respectively, resulting in the formation of a depletion region at certain points. The eddy current causes migration of the plasma particles from this region. This phenomenon may be called the "short circuiting effect" in the background plasma. As the density of the latter decreases, its

conductivity also decreases and, eventually, the short circuiting mechanism becomes ineffective. Therefore, as generally formulated, the problem is essentially nonlinear. An analysis of the simplest nonlinear problems of diffusion in an infinite plasma is presented in Refs. 57, 58. The foregoing effects are selectively disregarded in Refs. 11, 59-68 which analyze the evolution of the plasma perturbations. The applicability of the results of these articles is clearly limited.

The diffusion of a confined plasma was theoretically studied in many articles.^{41-43,69-74} In the case of an approximate solution of the problem of a plasma decay in a metallic chamber^{41,42} and also in the case of a numerical solution,⁴³ the potential profile was essentially postulated. This did not permit finding the correct potential profile in the plasma, and the boundary conditions were satisfied at four points only. In Ref. 74, which analyzes the stationary problem, the density profile was postulated and unrealistic boundary conditions were used. It was proposed to formally reduce the initial system of equations for the density and potential to a system of current equations.⁷¹⁻⁷³ However, this failed to lead to essentially new results. The effect of eddy currents on the evolution of the density profile in a dielectric apparatus was shown in terms of the relaxation of small deviations from the basic diffusion mode.⁷⁵ In the first (rapid) phase, eddy currents lead to a density redistribution in a plasma, resulting in ambipolar diffusion. The relaxation of eddy currents in a dielectric chamber with times substantially smaller than ambipolar was also uncovered through numerical calculations.⁶⁹

The solution of some of the simplest diffusion problems for a finite plasma is given in Ref. 76, where the boundary conditions, formulated in a companion work⁷⁷ for a plasma in a magnetic field, are used. Evidently, not only the nature of the bounding surface (metal or dielectric), but also the type of the boundary layer (diffusion or collisionless) exhibit considerable effect on the electric field in the plasma and on the nature of evolution of the plasma profile and lifetime.

A number of diffusion problems is encountered in the analysis of charged particle flows toward a solid placed in a plasma. The problem of a diffusion probe in a magnetic field is particularly interesting. In the one-dimensional case, the effect of the magnetic field is unimportant and the plasma density profile is defined by the ambipolar diffusion equation. A problem of this type was considered for a cylindrical probe placed along the magnetic field.⁷⁸ In the case of a probe of finite dimensions, Bohm had obtained expressions for the saturation currents.⁷⁹ A detailed theoretical study was made of the saturation current regime to a probe in the shape of an ellipsoid of revolution which was directed along the magnetic field.^{80,81} An experimental study of saturation currents in a finite-size probe and verification of Bohm's theory were carried out.⁸² The experimental results are in good agreement with theory. Values of the electron saturation current which substantially exceed theoretical ones were obtained.⁸³ The authors consider this divergence to be possibly the re-

sult of complex experimental geometry or charged particle production in a region near the probe. The analysis of an intermediate portion of the current-voltage characteristic, for which several authors have attempted to derive formulas,^{84, 85} is more complex. Numerical calculations show that for large values of probe potential, the potential profile in a plasma exhibits a quadrupole nature which corresponds to the short circuiting mode.⁸⁶ However, very small values of the magnetic field intensity, used in the calculations, have not provided the authors with an opportunity to study qualitatively any new features of the current-voltage characteristic which are dependent on the magnetic field. The solution of this problem is presented in Ref. 87.

4. DIFFUSION IN THE ABSENCE OF A MAGNETIC FIELD

In the absence of a magnetic field, the coefficients \hat{b}_α and \hat{D}_α are scalars.¹⁾ Having eliminated the electric field from Eqs. (1) and (2), we obtain the ambipolar diffusion equation [Eq. (15a)]:

$$\frac{\partial n}{\partial t} = D_a \Delta n.$$

But the electric field $\mathbf{E} = -\nabla\varphi$ is determined from Eq. (14).

$$\nabla (b_e + b_i) n \nabla \varphi = (D_e - D_i) \Delta n. \quad (17)$$

Several remarkable properties of Eqs. (15) and (17) should be noted. First of all, the equations for the density n and potential φ have been separated so that the density profile may be determined independently of the potential profile, i.e., $n(\mathbf{r}, t)$ is independent of currents passing through the plasma. Second, Eq. (15) for $n(\mathbf{r}, t)$ may be obtained by simply equating Γ_e and Γ_i so that if, for example, the components of Γ_e and Γ_i which are normal to the boundary are equal at the dielectric boundaries, $\Gamma_e = \Gamma_i$ holds over the entire volume. Third, the equations for ambipolar diffusion [Eq. (15a)] and field [Eq. (17)] are linear [for a given profile $n(\mathbf{r}, t)$].

However, it is evident that the nature of these properties is very special. We shall examine the simplest example in which N_0 "tagged" particles are injected into a small region of a homogeneous plasma of length l_0 and density n_0 in the absence of a magnetic field. Let, for the sake of simplicity, their mobility be equal to the mobility of the background particles, $T_e = T_i$, and the case be one-dimensional. The equations for the tagged $n_\alpha^{(p)}$ and background $n_\alpha^{(f)}$ particles coincide with Eqs. (1) and (2) and the quasineutrality condition is reduced to

¹⁾ If the plasma electrons are heated by the passage of an applied current, b_α and D_α are tensors, even in the absence of a magnetic field,⁸⁸ and phenomena, similar to those described below, are also possible in this case. However, the difference between the longitudinal and transverse (with respect to current) tensor components is normally small (of the order of unity) and they will be neglected here. In semiconductors, the tensor nature of b_α and D_α may be a function of crystal anisotropy.

$$n_0^{(p)} + n_e^{(f)} = n_i^{(p)} + n_i^{(f)}. \quad (18)$$

The evolution of the total plasma density profile $n(x, t)$ is expressed, as before, by Eq. (15a), and reduces to diffusion with the coefficient $D_a = 2D_i$. The solution of Eq. (15a) after a time interval $t \gg l_0^2/D_a$ is

$$n_{\text{amb}}(x, t) = n^{(p)} + n^{(f)} - n_0 = \frac{N_0}{\sqrt{4\pi D_a t}} \exp\left(-\frac{x^2}{4D_a t}\right), \quad (19)$$

$$\frac{e\varphi}{T} = \ln\left(1 + \frac{n_{\text{amb}}}{n_0}\right). \quad (20)$$

However, the total ambipolar diffusion profile with an effective width $\sim \Lambda_{\text{in}}$ is formed, in a complex way, as a result of the diffusion and field currents of the tagged and background particles. The linearity of Eq. (14) for the total density results from the precise compensation of nonlinear effects. If $n_\alpha^{(p)} \ll n_0$, the perturbed electric field is small and its inverse effect on the motion of the probing particles may be neglected; these particles drift in the unperturbed electric field and undergo diffusion with unipolar diffusion coefficients

$$n_\alpha^{(p)} = \frac{N_0}{\sqrt{4\pi D_\alpha t}} \exp\left[-\frac{(x \pm b_\alpha E_0 t)^2}{4D_\alpha t}\right]. \quad (21)$$

We shall first consider the case without an external current. The electric field and ion density are perturbed in a region of width $\sim \Lambda_{\text{in}}$. The profile $n_i^{(p)}(x, t)$ is defined by Eq. (21) and $n_i^{(f)} = n_{\text{amb}} + n_0 - n_i^{(p)}$ according to Eqs. (19) and (21). Moreover, the background ion density at $x=0$ is smaller than n_0 , since these ions are pulled out from there by the electric field and, therefore, form a depletion region as well as an ion perturbation component at the wings of the total profile (Fig. 2). If $n_i^{(p)} \gg n_0$, the problem becomes nonlinear for the probing particles. Since the total number of background ions in the perturbed region may not exceed $\sim n_0 \sqrt{4D_a t}$, the profile [Eq. (19)] consists mainly of tagged ions; the effect of the electric field associated with the latter is characterized by a $\sqrt{2}$ -fold broadening of the Gaussian profile [Eq. (20)]. As long as $N_0 \ll n_0 \Lambda_e$, Eq. (21) holds also for the tagged electrons. Moreover, N_0 injected electrons are distributed over a large area $\sim \Lambda_e$ and their contribution to the total profile [Eq. (19)] is insignificant. The profile almost entirely consists of the background electrons restrained by the electric field and collected as the result of unipolar diffusion from the depletion regions with an equivalent width $\sim \Lambda_e$. The maximum number of background electrons which may collect as a result of diffusion to form a perturbation is $\sim n_0 \Lambda_e$. If $N_0 > n_0 \Lambda_e$, the case for the probing electrons becomes strongly nonlinear. In es-

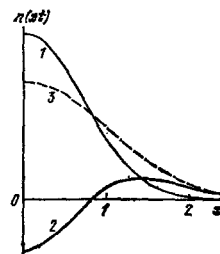


FIG. 2. Distribution of the probing (1) and background (2) ions and the total plasma density (3—ambipolar profile) for a point instantaneous source. Coordinate $x = \sqrt{4D_a t}$; small perturbation.

sense, the tagged particles undergo ambipolar diffusion. However, when

$$n_0 \Lambda_1 \ll N_0 \ll n_0 \Lambda_e, \quad (22)$$

nonlinearity of the probing electrons is intermediate. The electric field within the bounds of the ambipolar profile is, according to Eq. (20), large. Diffusion of the background and probing electrons proceeds at a rate essentially slower than the unipolar diffusion and the particles follow the Boltzmann distribution. Although the potential drop in this region is large and the inverse effect of the field on the motion of the probing electrons is considerable, the portion of the latter is the ambipolar profile associated with the intermediate nonlinearity is small (Fig. 3). The bulk of the probing electrons is confined to a region with the unipolar dimension $\sim \Lambda_e$ from which the electric field is absent.

The situation changes substantially in the presence of an external current. Figure 4 shows the behavior of the total density profile for the plasma (upper part) and for the tagged injected ions, whose mobility is equal to that of the background particles, in a plasma with a current. The magnitude of parameter A characterizes the nonlinearity of the initial profile. At small values of A , Eq. (19) holds and the plasma density is perturbed strictly by the background particles, —the probing electrons and ions are carried away in different directions by the current according to Eq. (21); moreover, the perturbation of their density is exactly compensated by the background plasma. If $n_{amb}(0, t) \geq n_0$, perturbation of the electric field is considerable. When

$$n_0 b_e E_0 t \gg 2N_0 \gg n_0 b_i E_0 t \quad (23)$$

the plasma density perturbation consists of the tagged ions and background electrons (intermediate nonlinearity). This situation is shown in Fig. 4 (lower part). Moreover, only a small fraction of the tagged ions is removed by the current; if, however, $2N_0 > n_e b_e E_0 t$, ambipolar diffusion of the tagged particles takes place (strong nonlinearity). If the mobility of the particles injected into a plasma with a current is different from the mobility of the background particles, in the case of a small signal two plasma perturbations occur: a stationary ambipolar bunch and a signal which travels with the drift velocity of the probing ions. The generation of the latter is attributed to the inability of the background plasma to screen out fully the perturbation of the probing ions as a result of different mobilities of the background and probing particles. If the

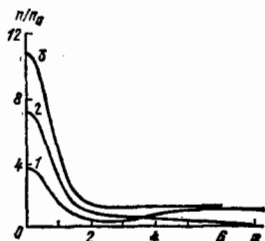


FIG. 3. Distribution of the probing (1) and background (2) electrons in a strongly nonlinear regime for a point instantaneous source. $D_e = 25D_a$, $n_{amb}(0, 0) = 11n_0$; 3—plasma density (ambipolar profile). Coordinate $x = \sqrt{4D_a t}$.

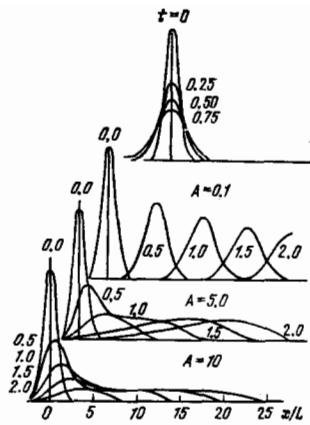


FIG. 4. Evolution of tagged ion profile in the presence of current.⁸⁹ Initial profile—Gaussian $n_1^{(0)} = A n_0 \exp[-x/L]^2$. Numbers by the curves—time in units of L^2/D_1 ; $eE_0 = 10AT/L$. Time, from which the tagged ions begin to be substantially carried away by the current is, according to Eq. (23), $t_{cr} \sim 5A$. Upper family of curves—total ambipolar profile.

background plasma consists of many components, the number of signals increases and, in the general case, there are $(K - 2)$ signals (K is the number of plasma components). The propagation of the signal at $K = 3$ is frequently encountered in semiconductor physics (electrons, holes and stationary charged centers); it is called ambipolar mobility.^{90, 91} Diffusion and recombination lead to attenuation of the perturbation.

5. SPREADING OF A DENSITY PERTURBATION IN AN INFINITE PLASMA IN A MAGNETIC FIELD

In a magnetic field, even in the case of a simple plasma with one kind of ions, the perturbations of the probing and background particle densities are not compensated. As a result of this, the total plasma density and potential are perturbed over a large volume, which corresponds to the propagation of the most mobile particles in a given direction. Moreover, the background particle drift is also uncompensated and the total plasma density decreases in certain regions. The separation of nonlinearity into strong and intermediate [Eqs. (22) and (23)] components which are associated with the strong or weak depletion of the background plasma, is also preserved in a magnetic field.

We shall first examine the evolution of a density perturbation against the background of an infinite homogeneous plasma.

a. Small perturbations without an external current

The simplest case is when the initial profile follows the sine curve with the wave vector \mathbf{k} .²⁰ Moreover, from Eqs. (1), (2) and (14), we obtain

$$\delta n(\mathbf{r}, t) \sim \exp[i\mathbf{k}\mathbf{r} - D(\mu^2)k^2 t], \quad (24)$$

where μ is the cosine of the angle between \mathbf{k} and \mathbf{H} , and

$$D(\mu^2) = \frac{[b_{e\parallel}\mu^2 + b_{e\perp}(1-\mu^2)][D_{i\parallel}\mu^2 + D_{i\perp}(1-\mu^2)] + [b_{i\parallel}\mu^2 + b_{i\perp}(1-\mu^2)][D_{e\parallel}\mu^2 + D_{e\perp}(1-\mu^2)]}{(b_{e\parallel} + b_{i\parallel})\mu^2 + (b_{e\perp} + b_{i\perp})(1-\mu^2)} \quad (25)$$

In the magnetic field which satisfies Eq. (7) we have

$$D(\mu^2) = \begin{cases} \left(1 + \frac{T_e}{T_i}\right) [D_{i\parallel} \mu^2 + D_{i\perp} (1 - \mu^2)] & \text{for } \mu \gg \mu_0, \\ \left(1 + \frac{T_i}{T_e}\right) [D_{e\parallel} \mu^2 + D_{e\perp} (1 - \mu^2)] & \text{for } \mu \ll \mu_0, \end{cases} \quad (26)$$

where $\mu_0 = \sqrt{b_{i\perp}/b_{e\parallel}} \ll 1$, i.e., $D(\mu^2)$ is identical with the smallest of the unipolar coefficients in the direction μ . At $\mu > \mu_0$, for example, diffusion is determined by the ions which flow at an angle γ with respect to H given by $\tan \nu = \sqrt{D_{i\perp}/D_{i\parallel}} \tan(\mathbf{k}, H)$. The electron diffusion flux along the magnetic field considerably exceeds Γ_i , so that regions with maximum plasma density are positively charged and the resultant electric field preserves quasineutrality; current flows in the plasma along constant density surfaces (perpendicular to the vector \mathbf{k}). At $\mu = \mu_0$, the electric field is entirely absent. Thus, in this simplest problem, plasma diffusion is essentially nonambipolar. By equating the fluxes $\Gamma_{e\parallel, \perp} = \Gamma_{i\parallel, \perp}$, instead of Eq. (26) we obtain

$$\bar{D}(\mu^2) \approx \left(1 + \frac{T_e}{T_i}\right) D_{i\parallel} \mu^2 + \left(1 + \frac{T_i}{T_e}\right) D_{e\perp} (1 - \mu^2). \quad (27)$$

This coefficient is considerably smaller than Eq. (26) and the difference is particularly significant at $\mu \sim \mu_0$. We should also note that in order to derive the ambipolar expression [Eq. (27)], a nonpotential electric field is needed. In other words, even if the plasma density depends on a single coordinate, the problem is not one-dimensional, i.e., particles fail to flow along \mathbf{k} and eddy currents are generated.

In the case of an arbitrarily small perturbation, Fourier expansion is applicable and the result formally comprises a superposition of expressions in Eq. (24). However, this gives rise to a qualitatively new effect which is associated with the multidimensionality of the problem. We shall examine the new effect in terms of the diffusion of a small point perturbation of density $\delta n(\mathbf{r}, t)$ (this corresponds to the Green's function for a diffusion problem).²⁰ The boundary and initial conditions are

$$\delta n(\infty, t) = n(\infty, t) - n_0 = 0, \quad \varphi(\infty, t) = 0, \quad \delta n(\mathbf{r}, 0) = N_0 \delta(\mathbf{r}). \quad (28)$$

The probing electrons injected into the plasma tend to occupy an ellipsoid with the semiaxes $\sim \Lambda_{e\parallel}$ and $\Lambda_{e\perp}$; the semiaxes of the ion ellipsoid are $\Lambda_{i\parallel}$ and $\Lambda_{i\perp}$, respectively. The resultant electric field near the origin of coordinates retards the most mobile particles in the corresponding direction: electrons along H and ions across H , i.e., at $\mathbf{r} = 0$, the potential has a saddle point. At $\mathbf{r} \rightarrow \infty$, the potential perturbation should be zero. Therefore, two symmetrical potential minima should be seen when $z = \mp z_0$, and at $\rho = \rho_0$ (ρ is a coordinate transverse to H) an annular maximum should occur in the plane $z = 0$, i.e., the field should be characterized by a quadrupole (Fig. 5). At $z > z_0$, the background electrons along H under the effect of the electric field should be channeled in the same direction as the diffused probing particles; at $\rho > \rho_0$, the electric field similarly enhances the diffusion flow of ions, the most mobile particles across H . Thus, in contrast to the case of diffusion in an isotropic plasma (Section 4), where the field and diffusion currents of the most mobile particles (electrons) outside the ambipolar re-

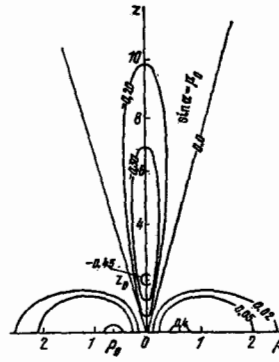


FIG. 5. Potential profile $\phi = e\varphi n_0 / TN_0 G(0, t)$ in the case of spreading of a point instantaneous perturbation in an isothermal plasma. Coordinate—in units of $\sqrt{8D_{i\parallel}t}$, $\Omega_e \nu_e = 30$, $\Omega_i \nu_i = 0.3$, $\alpha =$ angle between \mathbf{r} and H .

gion were fully compensated, in a magnetic field such compensation is impossible. The perturbed plasma occupies, roughly, a region which resembles two ellipsoids whose characteristic dimensions $\Lambda_{e\parallel, \perp}$ are defined by the unipolar coefficients of diffusion of electrons and ions (Fig. 6). In other words, a diffusion signal is propagated in almost the same manner as if the condition of quasineutrality did not exist at all. The electric field in a region which lies outside the "electron" and "ion" ellipsoids, causes the background particles to counterflow. The ions flow across H , into the electron ellipsoid and the background electrons, along H into the ion ellipsoid (Fig. 7). Quasineutrality is preserved by the flow of an eddy current in the background plasma. The potential perturbation vanishes at an angle $\sim \mu_0$ with respect to H ; the background particles drift away from here under the effect of the electric field and a depletion region is generated. The number of particles withdrawn from the depletion region is of the order of the total number of particles injected into the plasma. Numerical calculations confirm this inventory.^{54, 56}

The effective volume occupied by a perturbation in the absence of a magnetic field was of the order of $V_{\text{amb}} \sim \{D_{i\parallel} t [1 + T_e/T_i]\}^{3/2}$. However, in a magnetic field, the electron and ion ellipsoid volumes are $V_e \sim \Lambda_{e\parallel} \Lambda_{e\perp}^2$

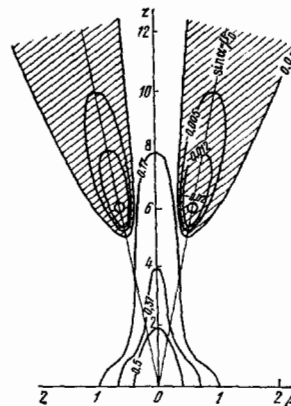


FIG. 6. Profile of density perturbation due to a point instantaneous source [Green's function $G(\mathbf{r}, t)$], relative to a value of perturbation at the origin of coordinates. Notation same as in Fig. 5; depletion region is cross hatched.

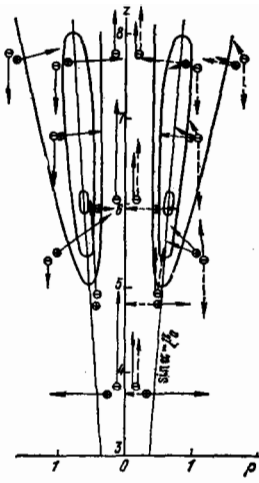


FIG. 7. Field and diffusion particle flows near the depletion region (see Fig. 6). Dashed arrows on the right-hand side indicate field flows, solid—diffusion flows, $\hat{D}_a \nabla n$; total flows are shown on the left-hand side.

$\sim D_{\parallel}^{1/2} D_{\perp} t^{3/2} [1 + (T_i/T_e)]^{3/2}$, and $V_i \sim \Lambda_{in} \Lambda_{iL}^2 \sim D_{\parallel}^{1/2} D_{iL} [1 + (T_e/T_i)]^{3/2}$. The ratio

$$\frac{V_{\text{omb}} + V_i}{V_{\text{omb}}} \sim \left(\frac{v_{\text{e}}}{\Omega_{\text{e}}}\right)^{1/2} \left(\frac{v_i}{\Omega_i}\right)^{3/2} + \frac{v_i^2}{\Omega_i^2 + v_i^2}. \quad (29)$$

characterizes the change in the effective volume filled by the plasma perturbation when a magnetic field is applied. Regardless of the reduction in the transport coefficients which follows, the volume occupied by a perturbation may substantially increase. The density at the origin of coordinates varies in accordance with the law⁵⁴

$$\frac{\delta n(0, t)}{n_0} \approx \frac{N_0}{n_0} (4\pi D_{\parallel} t)^{-3/2} \left(1 + \frac{T_e}{T_i}\right)^{3/2} \left[1 + \left(\frac{\Omega_i}{v_i}\right)^2 + \left(\frac{\Omega_e}{v_e}\right)^{1/2} \left(\frac{\Omega_i}{v_i}\right)^{3/2}\right]. \quad (30)$$

The above ratio is of the order of $(V_i^{-1} + V_e^{-1})N_0/n_0$, i.e., the density in the region where the ellipsoids overlap is determined by the volume of the smallest ellipsoid. Figure 8 shows the density profiles along rays emanating from the origin of coordinates. A relatively steep (with a scale length $\sim \Lambda_{e\parallel}$) plasma density gradient and an electric field which retards the more mobile particles (ions) occur at the boundary of the overlap region and the large (in this case, ion) ellipsoid. In other words, the density profile in the overlap region is ambipolar, i.e., it follows the Gaussian distribution with the

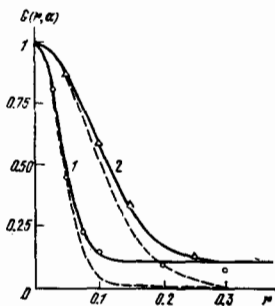


FIG. 8. Density profiles along straight lines inclined at an angle α to the magnetic field with $T_e = T_i$. 1— $\cos \alpha = 0$, 2— $\cos \alpha = 0.9$. Solid curves—approximate solution,⁵⁶ symbols—numerical calculations,⁵⁴ dashed lines—ambipolar Gaussian profile. Distance in units of $\sqrt{8D_{\parallel} t}$, $\Omega_i/v_i = 1$, $\Omega_e/v_e = 10^3/3$, $V_e/V_i \approx 0.11$. Boundary of the overlap region and ion (large) ellipsoid corresponds to $0 < \cos \alpha < 1 - D_{e\parallel}/2D_{i\parallel} \approx 0.999$.

diffusion coefficient $D_{e\parallel}[1 + (T_i/T_e)]$. The plasma density and potential, in a region corresponding to the electron and ion ellipsoids, are

$$\delta n(r, t) \approx n^{(e)} + n^{(i)}, \quad (31)$$

$$e\varphi(r, t) \approx T_e \ln\left(\frac{n^{(e)}}{n_0} + 1\right) - T_i \ln\left(\frac{n^{(i)}}{n_0} + 1\right), \quad (32)$$

where

$$n^{(e)} = \frac{N_0 \exp\left\{-\frac{z^2}{4D_{e\parallel}t[1+(T_i/T_e)]} - \frac{\rho^2}{4D_{e\perp}t[1+(T_i/T_e)]}\right\}}{\{4\pi t[1+(T_i/T_e)]\}^{3/2} D_{e\perp} D_{e\parallel}^{1/2}} \sim n_0 h \frac{D_{i\perp}}{D_{e\perp}}, \quad (33)$$

$$n^{(i)} = \frac{N_0 \exp\left\{-\frac{z^2}{4D_{i\parallel}t[1+(T_e/T_i)]} - \frac{\rho^2}{4D_{i\perp}t[1+(T_e/T_i)]}\right\}}{\{4\pi t[1+(T_e/T_i)]\}^{3/2} D_{i\perp}^{1/2} D_{i\parallel}} \sim n_0 h \sqrt{\frac{D_{e\parallel}}{D_{i\parallel}}}.$$

We shall assume $T_e = T_i$ and $D_{e\perp} \ll D_{i\perp}$. The asymptotic behavior of the density perturbation in this case is given, according to Ref. 56, by

$$\delta n(r, t) = N_0(G_1 + G_2),$$

$$G_1(r, t) =$$

$$\frac{D_{i\perp}}{2r^2 \mu_0^2} \cos^4 \alpha \frac{(9 \sin^4 \alpha / 2 \mu_0^2) - (36 \sin^2 \alpha / \mu_0^2) + 12}{[1 + (\sin^2 \alpha / \mu_0^2)]^{3/2}}, \quad (34)$$

$$G_2(r, t) =$$

$$\frac{9t D_{i\perp}}{2\pi r^3} \left(\frac{\mu_0 \cos^2 \alpha}{\sin^2 \alpha} + \frac{\mu_0}{\sin \alpha}\right) - \text{for } \sin \alpha > \mu_0,$$

and the asymptotic behavior of the potential $\varphi = (T_e/T_i)N_0(\Phi_1 + \Phi_2)$

$$\Phi_1 = \frac{(\sin^2 \alpha / \mu_0^2) - 2}{4\pi r^2 \mu_0^2 n_0 [(\sin^2 \alpha / \mu_0^2) + 1]^{3/2}}, \quad (35)$$

$$\Phi_2 = \frac{\mu_0}{4\pi n_0 r^3} - \text{for } \sin \alpha > \mu_0.$$

is characteristically quadrupole. A depletion region exists in the interval $\sin \alpha \sim \mu_0$ (see Figs. 6 and 7), with the relative depth h being of the order of the ratio of the number of the probing and background particles in the depletion region (its volume, however, is of the order of $\Lambda_{e\parallel}/\Lambda_{i\perp}$, i.e., it considerably exceeds the ellipsoid volume):

$$\frac{\delta n}{n_0} \sim N_0 [16 \sqrt{2} \pi^{3/2} t^{3/2} D_{e\parallel}^{1/2} D_{i\perp} n_0]^{-1} \equiv h. \quad (36)$$

These expressions hold outside the electron and ion ellipsoids. Since the potential is proportional to r^{-3} , the field currents obey $\Gamma_f \sim r^{-4}$. The density perturbation to which the latter give rise in accordance with $\partial n / \partial t \sim \nabla \Gamma_f$, is proportional to t/r^5 , i.e., it corresponds to Eq. (34). The diffusion currents $\sim r^{-6}$ are small compared to the field currents. Consequently, the density perturbation far from a source is caused by a redistribution of background particles, which is associated with the flow of an eddy conduction current.

The coefficient $D(\mathbf{k})$, determined from Eq. (25), is a function of $\mu = \cos(\mathbf{k}, \mathbf{H})$ only, i.e., at $\mathbf{k} = 0$, it is undefined and contains a singularity.²⁰ The presence of the latter is what leads to a nonGaussian asymptotic behavior with the depletion regions determined by Eqs. (34) and (35). Since the Fourier component of the perturbation with $\mathbf{k} = 0$ corresponds to a change in the total number of plasma particles. These effects are absent

²⁰The formulas for G_2 and Φ_2 are exhibited above only for $\sin \alpha > \mu_0$ since outside this region both G_2 and Φ_2 are small in comparison with G_1 and Φ_1 .

if the density perturbation is not accompanied by a change in the number of particles. Thus, for example, if the initial perturbation of the density is in the form of a Gaussian wave packet $\exp[i\mathbf{k}_0 \cdot \mathbf{r} - (\nabla \mathbf{k}, \mathbf{r})^2]$; $\Delta k \ll k_0$, i.e., the perturbation of the total number of particles is small, $\sim \exp[-(k_0/\Delta k)^2]$, then both the depth of the depletion regions and the asymptotic behavior given by Eqs. (34) and (35) are proportional to this small multiplier.⁵⁶ The wave packet itself attenuates as $\exp[-D(k_0)k_0^2 t]$.

If the perturbation is finite, a one-dimensional ambipolar mechanism may be important in certain regions. Thus, for example, if the initial perturbation extends along the magnetic field, the eddy current in the background plasma causes a rapid unipolar spreading of the tails of the perturbation. The middle portion, however, undergoes an ambipolar spreading, i.e., its width increases as $\sqrt{D_{e\perp} t}$. The perturbation takes on the bell shape, and if we have

$$\frac{L_{\parallel}}{L_{\perp}} > \sqrt{\frac{D_{e\parallel}}{D_{e\perp}}}, \quad (37)$$

then the diffusion unipolar signals from the end regions fail to merge before the one-dimensional ambipolar diffusion becomes significant (Fig. 9).

b. Evolution of a nonlinear perturbation

In the linear case, the density perturbation within the electron and ion ellipsoids considerably ($D_{\perp\perp}/D_{e\perp}$ - and $\sqrt{D_{e\parallel}/D_{i\parallel}}$ -fold, respectively) exceeds the maximum value of the perturbation in other regions, so that the nonlinear effects should occur, first of all, in the ellipsoids. In this region the solution is⁵⁷

$$\delta n = n - n_0 = n^{(e)} + n^{(i)} + h n_{\text{amb}}, \quad (38)$$

where $n^{(e)}$ and $n^{(i)}$ are expressed by Eq. (33) and

$$n_{\text{amb}}(r, t) = N_0 \exp\left(-\frac{r^2}{4D_{e\parallel} t} - \frac{\rho^2}{4D_{a\perp} t}\right) (16\sqrt{2}\pi^{3/2}t^{3/2}D_{i\perp}^{1/2}D_{e\perp})^{-1} \\ = h n_0 \frac{D_{i\perp}}{D_{e\perp}} \sqrt{\frac{D_{e\parallel}}{D_{i\parallel}}} \exp\left(\frac{r^2}{4D_{e\parallel} t} - \frac{\rho^2}{4D_{a\perp} t}\right) \quad (39)$$

is the ambipolar solution.

The density perturbation outside the ellipsoids is small, yielding a linear solution. The area in which Eq. (38) is applicable is strictly limited by the condi-

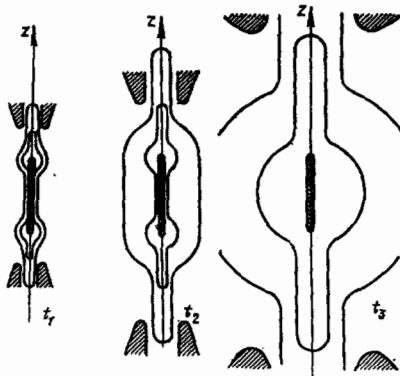


FIG. 9. Spreading of a linear plasma perturbation, highly stretched along the magnetic field ($L_{\parallel}/L_{\perp} \gg \sqrt{D_{e\parallel}/D_{e\perp}}$). Initial perturbation is shown cross hatched. $t_1 < t_2 < t_3$.

tion $h \ll 1$. Thus, it correctly describes not only small ($\delta n \ll n_0$) perturbations but also comparatively large plasma inhomogeneities, where the density inside the ellipsoids exceeds n_0 many times, i.e., an intermediate nonlinearity regime. In the ellipsoid overlap region an ambipolar peak occurs with $n \sim n_0 h^2 (D_{\perp\perp}/D_{e\perp}) \sqrt{D_{e\parallel}/D_{i\parallel}}$, which contains a small fraction (of the order of h) of the total number of injected particles. Diffusion inside this peak is determined by the ambipolar mechanism, so that the electron and ion currents are identical everywhere. Outside the peak, expressions for the currents in the electron and ion ellipsoids and, consequently, the density profile [Eq. (38)] are the same as in the linear case. Thus, as long as the relative depth of the depletion regions remains small, the short-circuiting mechanism for currents in the background plasma remains in effect. It provides a possibility for the injected particles to spread with unipolar velocity due to arrival of electrons and ions from the depletion regions. When the background plasma is considerably depleted (strong nonlinearity, $h > 1$), the nature of the solution undergoes a substantial change. Moreover, the number of particles in the central peak approaches the total number of particles injected into the plasma, and the density is expressed by Eq. (39), i.e., a perturbation basically evolves in an ambipolar manner. Only a small portion of particles spreads into the electron and ion ellipsoids due to the short-circuiting mechanism. The density in the ellipsoids may be estimated knowing the characteristic dimensions of the region from which the lacking particles come to preserve quasineutrality. Background plasma ions can enter the electron ellipsoid coming across the magnetic field from distances of the order of $\Lambda_{i\perp}$, so that the number of ions assembled in the electron ellipsoid volume is $\sim n_0 \Lambda_{e\parallel} \Lambda_{i\perp}^2$, and the plasma density in it is

$$\delta n^{(e)} \sim \frac{n_0 D_{\perp\perp}}{D_{e\perp}}. \quad (40)$$

The plasma density in the ion ellipsoid is similarly estimated by

$$\delta n^{(i)} \sim n_0 \sqrt{\frac{D_{e\parallel}}{D_{i\parallel}}}. \quad (41)$$

The background ions accumulated in the electron ellipsoid are held in it by a strong transverse electric field which falls off with the decrement $\Lambda_{e\parallel}$. This leads to a strong depletion of the background plasma near the ellipsoid, and the transverse diffusion broadens the size of the depletion region to $\Lambda_{r\parallel}$. The motion of the background electrons proceeds similarly. The spreading of nonlinear perturbations of finite dimensions was studied numerically by Voskoboïnikov and coworkers.⁵⁸

The asymptotic behavior $\delta n \sim t/r^5$ and $\varphi \sim r^{-3}$ applies outside the ellipsoids. Moreover, at $h > 1$ the density perturbation at the edge of this region should be of the order of n_0 , so that the asymptotic behavior is

$$\delta n(r, t) \sim \frac{\delta n_{i1n}(r, t)}{h},$$

where δn_{i1n} is the corresponding expression in the linear case.

In the case of a perturbation of an arbitrary shape which considerably exceeds n_0 , the effect of the back-

ground plasma is insignificant. However, the short-circuiting mechanism may be effective inside the plasma bunch. It should lead rather quickly to the establishment of the profile $n_1(z)n_2(\rho)$ which constitutes the initial condition for the ambipolar diffusion (in similarity with the profile evolution in a dielectric container, see below).

Above, we have examined a positive perturbation of the plasma density. However, in the case of negative perturbations of small size, the short-circuiting mechanism is always effective since $|\delta n|/n_0 \lesssim 1$.

A number of nonlinear effects may be associated with the dependence of \hat{D}_e and \hat{b}_e on the plasma density due to electron-ion collisions [Eqs. (12) and (13)]; however, we shall not consider these in this review.

c. Allowance for an external current

Let the spatially-homogeneous current density \mathbf{j} [or the field \mathbf{E} , such that $\mathbf{j} = (\hat{b}_e + \hat{b}_i)n_0\mathbf{E}$] be prescribed at infinity. The flow of an external current in a magnetic field (as also the presence of ions of various kinds; Section 4) results in a small perturbation with the wave vector \mathbf{k} in an isothermal plasma propagating with the phase velocity

$$V(\mu^2) = \frac{c}{T} \frac{[D_{e\parallel}\mu^2 + D_{e\perp}(1-\mu^2)]\hat{D}_iE - [D_{i\parallel}\mu^2 + D_{i\perp}(1-\mu^2)]D_eE}{(D_{e\parallel} + D_{i\parallel})\mu^2 + (D_{e\perp} + D_{i\perp})(1-\mu^2)}. \quad (42)$$

The above quantity is called ambipolar drift velocity^{20, 54} (see also Refs. 11, 92). The wave packet propagates accordingly with the group velocity

$$V_{gr}(\mu^2) = \frac{\partial}{\partial \mathbf{k}}(kV(\mathbf{k})), \quad (43)$$

and it spreads as a result of diffusion with the coefficient $D(\mu^2)$. The phase and group velocities (as well as D) depend on $\mu = \cos(\mathbf{k}, \mathbf{H})$ only, so that at $\mathbf{k} = 0$ both are indefinite. Therefore the Fourier component of perturbation corresponding to $\mathbf{k} = 0$ (i.e., perturbation of the total number of plasma particles), behaves entirely differently. Similarly, as in the absence of a current, particle injection results in the flow of eddy currents in the plasma and in the formation of depletion regions, although the processes evolve in a more complex manner in this case.^{20, 56} In the initial stages of evolution the perturbation is determined by diffusion, so that the situation is identical with the one described above. However, at later stages the dispersion mechanism for the spreading of an inhomogeneity becomes important the phase velocity [Eq. (42)] being a function of the wave vector \mathbf{k} .²⁰ This leads to two effects: the disintegration of the perturbation into several bunches and an increased rate of their spreading compared to the diffusion rate. The maximum perturbation occurs along the extremal curve^{20, 3)} which is expressed by the following equation:

$$\mathbf{r} = V(\mu_m^2)t, \quad (44)$$

where μ_m takes on all values between zero and unity. There are three plasma bunches in the vicinity of the

points

$$\mu_m^2 = 0, \quad \mu_m^2 = 1 \quad \text{and} \quad \mu_m^2 = \frac{\mu_0^2 E_1^2}{E_0^2 + \mu_0^2 E_1^2} \quad (45)$$

(Fig. 10, bunches A, B, C). The amount of excess plasma in each bunch is of the order of the total number of particles injected into the plasma. In the case of the first bunch, the component velocities along the magnetic field and in the direction $[\mathbf{E}, \mathbf{H}]$ coincide (with an accuracy up to small terms) with the electron speed and, therefore, it may be conventionally called an electron bunch. The velocity of the second bunch across \mathbf{H} approaches the ion speed, so that it may be called an ion bunch. We should note, however, that neither the velocity nor the dimensions of the bunches coincide with the velocities and dimensions of the probing particle clusters. The position of the third bunch corresponds to the point of contact between the group velocity surface $\mathbf{r} = V_{gr}(\mu^2)t$ and the extremum line. The perturbation along the latter between the first and third bunches is positive, and between the second and third, negative (see Fig. 10). If $\mathbf{E} \parallel \mathbf{H}$ or $\mathbf{E} \perp \mathbf{H}$, bunch A merges with bunch B or C . The process of "disintegration" of the diffusion profile into traveling plasma bunches was studied numerically in both cases ($\mathbf{E} \parallel \mathbf{H}$ and $\mathbf{E} \perp \mathbf{H}$).^{20, 56}

The potential perturbation is dipole in nature $\varphi \sim r^{-2}$, so that the asymptotic behavior of the density perturbation, proportional to t/r^4 depends on the redistribution of background particles under the action of the perturbed electric field.

If, for example, the mobilities of the injected and background ions are different, as is the case in the ionospheric bariated clouds, the counterflow of background ions fails to compensate fully the density perturbation in the region into which the probing tagged particles flow. Under these circumstances, we have one more plasma density extremum.⁵⁶

An increase in $\delta n/n_0$ leads to a number of nonlinear effects. The simplest is a solution of the plane problem, where the perturbation is a function of a single coordinate ξ . Moreover, regardless of the magnitude of the perturbation, the density equation is linear

$$\frac{\partial n}{\partial t} = D(\bar{\mu}^2) \frac{\partial^2 n}{\partial \xi^2} - V_z(\bar{\mu}^2) \frac{\partial n}{\partial \xi}, \quad (46)$$

where $\bar{\mu}$ is the cosine of the angle between \mathbf{H} and ξ , V_z

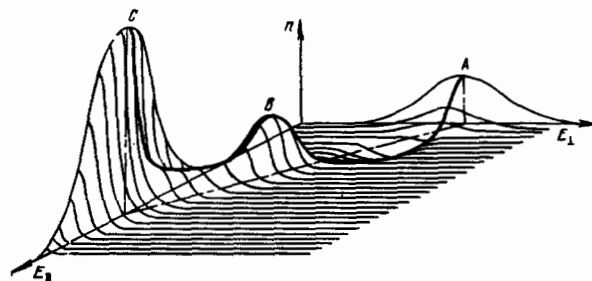


FIG. 10. Schematic model of spreading of a small point perturbation of plasma density with an external current near the extremum curve. B —electron cluster, C —ion cluster, z -axis—along the magnetic field (cluster motion in the direction $[\mathbf{E}, \mathbf{H}]$ not shown).

³⁾In the absence of electron-ion collisions, within an accuracy up to the small terms, $D_{e\perp}/D_{i\perp}$, $D_{i\parallel}/D_{e\parallel}$: this curve is a straight line.

is the projection of Eq. (42) onto ξ and $D(\mu^2)$ is defined by Eq. (25).

In the case of a nonlinear perturbation of finite size the situation is considerably different, depending on how effective is the mechanism for the short circuiting of flows in the background plasma. If the initial size of the perturbation is small, the only significant parameter is the relative depth of the depletion regions

$$h \sim \{D_{e\parallel} (E_{\parallel} + E_{\Delta})^2 D_{i\perp} [D_{i\perp} (E_{\parallel} + E_{\perp}) + (D_{ed} - D_{id}) E_{\perp}] \}^{-1} \frac{N_0}{n_0}. \quad (47)$$

At $h < 1$, the density profile is the same as in the linear case, although the perturbed density may appreciably exceed n_0 . And the perturbation of the potential near the maxima A , B and C is

$$\varphi(r, t) = \varphi_{lin}(r, t) \frac{n_0}{\delta n_{lin}(r, t)} \ln \frac{n(r, t)}{n_0}. \quad (48)$$

where r , corresponds to the coordinates of the maxima of [Eq. (45)]. Moreover, the field current expressions coincide with the results of the linear theory: $n_0 \nabla \varphi_{lin} = n \nabla \varphi$. There is no ambipolar peak.

If, however, $h > 1$, currents in the background plasma are insignificant and ambipolar diffusion is basically responsible for spreading; the background plasma density is insufficient to produce short circuiting and the injected particles occupy an ellipsoid with the semi-axes $\Lambda_{i\parallel}$ and $\Lambda_{e\perp}$ near the origin of coordinate, i.e., the external field is practically totally screened by the plasma. But, a small fraction of particles (of the order of h^{-1}) injected into the plasma may, as before, move unipolarly to form the "sleeves" OA , OB and AC .

d. Spreading of a plasma pinch

In the case of a small density perturbation the solution is a two-dimensional analog of the point source problem which was considered above. The density perturbation (in the plane xOz' , perpendicular to the pinch) is considerable in the region formed by the superposition of two ellipses, the electron ellipse with the semi-axes $\Lambda_{e\perp}$ and $\tilde{\Lambda}_{e\parallel}$ and the ion ellipse, with the semi-axes $\Lambda_{i\perp}$ and $\tilde{\Lambda}_{i\parallel}$. Equation (8) is used to determine $\tilde{\Lambda}_{e\parallel}$, with the following substitution for $D_{e\parallel}$

$$\tilde{D}_{e\parallel} = D_{e\parallel} \sin^2 \theta + D_{e\perp} \cos^2 \theta, \quad (49)$$

where θ is the angle between the pinch axis and the magnetic field. The asymptotic behavior of the perturbation and the location of the depletion regions may be obtained from Eq. (34).⁹³ Figure 11 schematically shows the geometry of a pinch. If the angle of dip θ is small ($< \mu_0 = \sqrt{D_{i\perp}/D_{e\parallel}}$), then $\tilde{\Lambda}_{e\perp} < \tilde{\Lambda}_{i\parallel}$, the depletion regions vanish and the diffusion becomes ambipolar (in both linear and nonlinear cases). The dimensions of the perturbed region are, furthermore, sharply reduced (to $\tilde{\Lambda}_{e\parallel}$, $\Lambda_{e\perp}$).

In the case of a strong density perturbation, the Hall currents which occur during diffusion may become substantial in the electric field and be of the order of the nonlinear effects examined above. Since these currents in a strong magnetic field are $\sim H^{-1}$ (and the diffusion coefficient across the magnetic field is $\sim H^{-2}$), an opinion was expressed that they can greatly ac-

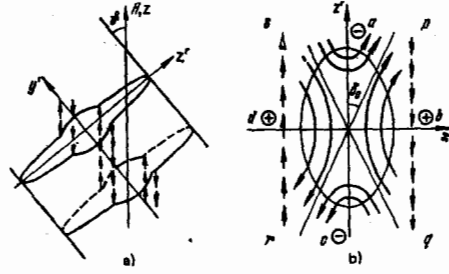


FIG. 11. Spreading of a plasma pinch for $\theta > \min(\sqrt{\mu_0}, \nu_i/\Omega_i)$. Small arrows indicate electron flows along H which short circuit the Hall current; right-hand side (b) shows the ambipolar ellipse; s, q —positive space charge, p, r —negative space charge.

celerate transport across H .⁷⁰ However, the effect is actually considerably more complex. At $\theta > \min[\nu_i/\Omega_i, \sqrt{\mu_0}]$, the Hall currents are "short circuited" by the electron and ion currents along and across H , respectively, and the situation, as before, is similar to the case of a point perturbation. At $h = N_0 / (8\pi n_0 \sqrt{D_{i\perp} \tilde{D}_{e\parallel}}) < 1$ (N_0 is the number of injected particles per unit length of the plasma pinch), the short-circuiting mechanism is in effect, and at $h \gg 1$, ambipolar diffusion takes place. Actually, the constant density and potential surfaces in the electron and ion ellipses coincide, so that the Hall currents fail to cause changes in the plasma density. Outside the ellipses, however, the density and potential are only slightly perturbed. Therefore, the Hall currents may have an appreciable effect only in a region where the ellipses overlap, i.e., in the ambipolar ellipse. If these currents were not taken into account, the plasma would be polarized as a quadrupole ($abcd$ in Fig. 11b). The maximum divergence of the Hall current in this field (thin lines in Fig. 11b) occurs in the directions which form an angle $\delta_0 = \sqrt{D_{e\perp}/\tilde{D}_{i\parallel}}$ with the z' -axis (the angle between the currents and constant density lines is almost 90° in this case) and is $\sim b_{e\perp}(\Omega_e/\nu_e)n(0)\varphi(0)/(\Lambda_{e\perp}\tilde{\Lambda}_{i\parallel})$. The resultant polarization ($pqrst$) leads to the flow of electrons and ions along and across H , respectively. The divergence of the electron flow, determined by the potential $\delta\varphi$ with this polarity, is $\sim b_{e\parallel}n\delta\varphi\theta^2/\Lambda_{i\parallel}^2$. Therefore, at $\theta > \sqrt{\mu_0}$, $\Omega_i < \nu_i$, a small perturbation $\delta\varphi \sim \varphi(0)\mu_0/\theta^2$ is sufficient to compensate the divergence of the electron Hall current. The ion Hall current is similarly short circuited across H at $\Omega_i > \nu_i$.

The nature of evolution of a nonlinear perturbation should be substantially changed by the drift in the crossed fields only at angles $\mu_0 < \theta < \theta_0 = \min[\nu_i/\Omega_i, \sqrt{\mu_0}]$. The ongoing processes resemble the widely known phenomenon of the reestablishment of conduction across the magnetic field, under the conditions where the Hall current is forbidden. The polarization ($pqrst$, see Fig. 11b) cannot now be "shorted" along H , and new Hall currents appear in this field. Their divergence (on the scale of the ambipolar ellipse) $\sim e\delta\varphi D_{ed}/(T\Lambda_{e\perp}\tilde{\Lambda}_{i\parallel})$ (at $\Omega_i < \nu_i$) is small compared to $\text{div } \Gamma_{e\parallel}$, but exceeds $\text{div } \Gamma_{i\parallel}$. Therefore, the electric field across H should change sign and the transverse dimension of a strong perturbation increases from $\Lambda_{e\perp}$

to Λ_{iH} . The potential profile, moreover, should correspond in the first approximation to the Boltzmann electron distribution, such that the Hall currents pass along the constant density surface. And the small "bending" of the polarization ($pqrs$) is determined by the condition requiring that the electron Hall current be equal to $\Gamma_{iH} - \delta\varphi \sim (T/e)D_{iH}/D_{ed}$. At $\Omega_i > \nu_i$, the ion Hall current is somewhat smaller (by an amount of the order of $\sim \nu_i^2/\Omega_i^2$) than the electron Hall current. Therefore, the diffusion flow of ions across H has to compensate this small difference only. The transverse scale in this case also equals Λ_{iH} .

A numerical calculation of the spreading of a plasma pinch of finite initial dimensions and oblique to H was carried out for a broad range of angles ϑ .⁹² At the onset, the maximum density was three times greater than the background density, which corresponds to intermediate nonlinearity. The potential formed a quadrupole; at large ϑ , its extrema were located practically on the x and z' axes and the density profile was symmetrical with respect to x and z' . This confirms the minor role of the Hall currents. However, a considerable "bending" of the density and potential profiles was observed at small ϑ (Fig. 12).

Since the Hall current effect may be important in the regions where the perturbed density considerably exceeds background, profile "bending" in the peripheral regions was small. The value of μ_0 was nearly 1° and $\vartheta_0 \sim 7^\circ$. The rate of decrease of density along the axis increased sharply when ϑ changed from 0 to 1° . The rise is slowed down when $1^\circ < \vartheta < 5^\circ$. And changing from 5° to 90° ; had practically no effect on the rate of decrease of density. This is in agreement with the model presented above.

e. Experiments in the ionospheric plasma

The substance in which the effects described above play a major role is the ionospheric plasma. Actually, in the geomagnetic field $\rho_e < \lambda_e$, starting at altitudes ≤ 80 km, and $\rho_e \rho_i < \lambda_e \lambda_i$ above ~ 95 km; the effect of collisions between charged particles on the diffusion is insignificant up to ~ 300 km. Precisely in this region, intensive studies of meteor tracks, bariated clouds,

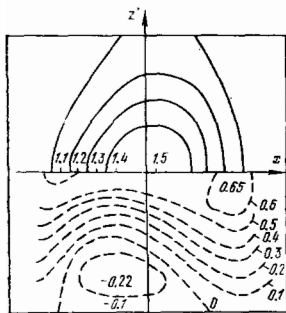


FIG. 12. Numerical calculation of spreading of a plasma pinch inclined at the angle $\vartheta = 1^\circ 50'$ to H. Parameters correspond to ionosphere at an altitude of 102 km. Initial profile—Gaussian: $\delta n(x, 0) = 2n_0 \exp[-0.6(x^2 + y^2)/R^2]$. Coordinates in units of R , $t = R^2/2D_{iH}$. Upper half—density profile $\delta n/n_0$; lower half—potential profile in units of $T/10e$.

evolution of the natural plasma inhomogeneities, rocket and satellite tracks, etc., are continuing. In a large number of cases the effect of the background plasma inhomogeneity and of boundaries is not very significant. Unfortunately, information concerning the plasma perturbations caused by these effects is very incomplete. In particular, studies of the bariated clouds normally focus on the behavior of the "tagged" barium ions only, whereas it follows from the foregoing that the nature of the background plasma perturbation is more complex and involves a much larger volume. The concurrent studies of the evolution of "tagged" ions and of the background plasma may, in principle, yield considerably greater information concerning the condition of the ionosphere. An indirect confirmation of the above model of the short circuiting of eddy currents in the background plasma may be perceived from a number of experimental facts. Thus, for example, Fig. 13 shows the time dependence of the total number of barium ions determined photometrically from the cloud image.⁹⁴ The sharp falling off, recorded at $t_0 \sim 400$ sec, may be interpreted as follows. The concentration of Ba^+ ions at the initial stage of spreading exceeds the background 20-fold, which corresponds to intermediate nonlinearity. The ions were magnetized and, in the initial stages, one-dimensional ambipolar diffusion of the Ba^+ ions along H had taken place. However, the transverse motion of the Ba^+ ions could be associated only with the external electric field E in a system of coordinates which travels with the neutral gas. Since the electron and ion mobilities are different, charge separation occurs. The injected cloud of dense plasma can move in the direction [EH] only if the background ion flow can compensate this difference. Such motion, accompanied by a large increase in the cloud volume and a decrease in the Ba^+ ion concentration due to the dispersion mechanism of spreading,²⁰ become possible only if the displacement of the background ions along E_1 is comparable to the initial transverse dimensions. Assuming $E_1 \sim 2mV/m$ and $l_0 \sim 1$ km, we obtain $t_0 = l_0/b_{iH}E_1 \sim 400$ s. At $t > t_0$, the original cloud having the shape of an ambipolar ellipsoid at first, acquires a "tongue" which stretches in the direction [EH], whose dimensions rapidly grow with time.⁹⁵

In the course of experiments⁹⁶ carried out with large barium charges (> 1.8 kg), the nature of evolution was highly dependent on the number of Ba^+ ions (Fig. 14). The initial amount of barium ions in three clouds was estimated at $(0.7-2) \times 10^{23}$ (a 30-100-fold higher concentration than the background). These clouds moved

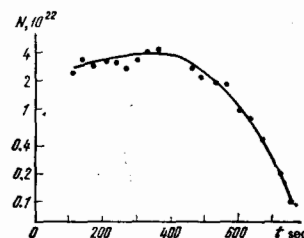


FIG. 13. Variation with time of the total number of the Ba^+ ions in a cloud.

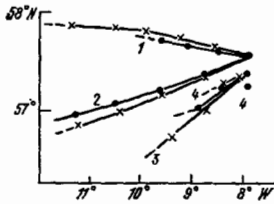


FIG. 14. Trajectory of neutral (circles) and ionized (crosses) barium clouds from data of Ref. 96.

practically together with the neutral clouds. The speed differential was not more than 10% and was smallest for the largest cloud (2). The latter moved together with a neutral cloud during the entire period of observation (~16 min). Two smaller clouds (1 and 3) were under observation for a shorter period (5–12 min). Toward the end of the observation period, the path of one of the clouds sharply deviated from the path of a neutral cloud. The fourth cloud contained roughly $(0.4-1.2) \times 10^{22}$ ions, which corresponded to an initial concentration at the center of $(2-6) \times 10^6 \text{ cm}^{-3}$ and exceeded only slightly the background concentration at these altitudes. Its speed at the onset had nothing in common with the speed of the neutral cloud. These facts are in qualitative agreement with the model presented above. The sharp changes in the direction of propagation of the ion clouds (including reverse propagation), observed in Refs. 97 and 98, are possibly also associated with the phenomena discussed above, and are dependent on the fact that a high-density cloud, moving with the wind at first, begins to move in the direction $[\mathbf{E}, \mathbf{H}]$ when the short circuiting mechanism is "switched on."

6. DIFFUSION OF PLASMA IN A FINITE VOLUME

a. Effective boundary conditions

An analysis of diffusion of a finite plasma requires that boundary conditions be defined for the density and the potential. If the thickness of the space charge layer, in which quasineutrality is violated, is small compared to the plasma dimensions, it is feasible to consider a solution in it as an effective boundary condition for the plasma quasineutral equations. The geometry of the boundary region may be considered plane and the number of particles in it small, so that the particle accumulation and ionization in that region are insignificant. Then the electron and ion currents, which flow in the region and are normal to the boundary, are preserved. Having expressed the currents in terms of the potential drop in this region, relations may be obtained which couple the particle current values (i.e., the potential and density derivatives normal to the boundary) to the values of potential and density at a certain boundary which is located sufficiently close to the plasma boundary. Let, for example, the boundary surface absorb all the incident particles, emission be nonexistent and the boundary potential with respect to the plasma be negative. If the layer thickness is less than λ_e (a collisionless layer), then in the case of Maxwellian distribution the electron current onto a boundary perpendicular to \mathbf{H} is

$$\Gamma_{e\perp} = \frac{1}{4} n(\Delta) \bar{v}_e \exp\left(-\frac{e\varphi(\Delta)}{T_e}\right); \quad (50)$$

where $\bar{v}_e = \sqrt{8T_e/\pi m_e}$ and $n(\Delta)$ and $\varphi(\Delta)$ are the values of the density and the potential at any point $z = \Delta$ in the boundary region where the geometry may be considered one-dimensional. The density profile near the boundary is linear and, if the coordinate of the conventional boundary surface is chosen to be $\Delta \gg \lambda_e, \lambda_i$, the density at the layer boundary may be taken as zero,¹⁰⁰ and Eq. (2) yields

$$n(\Delta) = -\frac{\Gamma_{e\perp} b_{i\parallel} + \Gamma_{i\parallel} b_{e\perp}}{D_{e\perp} b_{i\parallel} + D_{i\parallel} b_{e\perp}} \Delta. \quad (51)$$

The layer structure and the solution in the intermediate region were the subject of detailed discussions.^{101,102} The conditions of Eqs. (50) and (51) couple the values of the functions n and φ and their normal derivatives $\Gamma_{e\perp}$ and $\Gamma_{i\parallel}$ at the plasma surface located at a distance Δ from the boundary, i.e., they represent two mixed nonlinear boundary conditions for a quasineutral system of equations. In a magnetic field the length of time an electron spends in orbits, from which removal to a wall parallel to \mathbf{H} is possible, is short, i.e. of the order of Ω_e , and the orbits are filled as the result of relatively rare collisions.¹⁰³ The orbits are, therefore, practically vacant [to within $(\Omega_e/\nu_e)^{-1}$] and the electron current to the wall corresponds to the number of collisions which transfer the electrons from filled orbits to vacant ones. Consequently, \bar{v}_e in Eq. (50) must be replaced by $\bar{\rho}_e \bar{v}_e$, where $\bar{\rho}_e = \sqrt{2e\Delta\varphi_w/m_e}$ is the Larmor radius of an electron with energy $e\Delta\varphi_w$, \bar{v} is a properly averaged electron collision frequency,^{77,104} and $\Delta\varphi_w$ is the potential drop in the space charge layer.

$$\Gamma_{e\perp} = \frac{1}{4} n(\Delta) \bar{\rho}_e \bar{v}_e \exp\left(-\frac{e\varphi(\Delta)}{T_e}\right). \quad (50a)$$

If the layer thickness exceeds λ_n (or ρ_n), the diffusion equations are applicable also inside the layer, and $n_e = n_i = 0$ at the boundary. A numerical solution of this problem was presented by Su¹⁰⁵ and Cohen,¹⁰⁶ and simple analytical expressions, for the case where the drop in the layer substantially exceeds T_e and T_i , were obtained by Rozhanskii.⁷⁷ The phenomena associated with the dependence of ion mobility on electron field intensity and non-Maxwellian electron distribution function in a boundary region were discussed in detail elsewhere.^{101,102}

b. Diffusion in a dielectric apparatus

Our discussion of diffusion mechanisms shall be limited to the simplest problem concerning decay of a plasma inhomogeneous in two dimensions in a cylindrical vessel with walls parallel to the magnetic field. The Hall currents in this case flow along the constant density surface and have no effect on the diffusion. A case in which the inequalities $\tau_{e\perp} \ll \tau_{e\parallel}$ and $\tau_{i\parallel} \gg \tau_{i\perp}$ are satisfied for the fast and slow time scales of Eqs. (9) and (11), is particularly interesting. In the opposite case, ambipolar diffusion simply takes place since the short-circuiting processes, which correspond to the greatest of the fast times $\tau_{e\parallel}$ and $\tau_{i\perp}$, do not have time to occur during the time of ambipolar diffusion (the least of the slow times). We shall assume that the characteristic dimensions of the initial perturbation $n_0(r, z)$ are of the order of the apparatus dimensions (spreading of small-scale perturbations occurs in the

same manner as in an infinite plasma). We shall show that the evolution of any initial profile occurs in two stages. At first, rapid density redistribution occurs during a time of the order of the fastest time. Subsequently, the second (ambipolar) stage begins for which the electron and ion currents are equal throughout the plasma volume.

The analysis is simple for the limiting cases where either $\tau_{e||} \ll \tau_{i\perp}$ (short apparatus) or $\tau_{e||} \gg \tau_{i\perp}$ (long apparatus). The electric field in a short apparatus corresponds to a Boltzmann distribution of electrons along H:

$$\varphi(r, z, t) = \frac{T_e}{e} [\ln n(r, z, t) + \psi(r, t)]. \quad (52)$$

If we neglect the longitudinal ion diffusion and integrate the equation for the ions along the length of the apparatus, we obtain

$$\frac{\partial N_1}{\partial t} = \frac{1}{r} \frac{\partial}{\partial r} r D_{i\perp} \left[\left(1 + \frac{T_e}{T_i} \right) \frac{\partial N_1}{\partial r} + N_1 \frac{T_e}{T_i} \frac{\partial \psi}{\partial r} \right], \quad (53)$$

where $N_1(r, t)$ is the number of plasma particles in a cylindrical layer of unit cross section, which is parallel to H and abuts against the ends of the apparatus. The boundary condition requires that the normal components of the fluxes to the wall be equal, i.e., $\Gamma_{e\perp} = \Gamma_{i\perp}$. Therefore, particle removal is determined by the slow times and, in the fast stage, we may assume $\partial N_1 / \partial t = 0$ and $\Gamma_{i\perp} = 0$.

It follows from Eq. (53) that

$$\frac{\partial \psi}{\partial r} = -\frac{\partial}{\partial r} [\ln N_1(r, 0)] \left(1 + \frac{T_i}{T_e} \right), \quad (54)$$

and the plasma density equation for the fast stage becomes

$$\frac{\partial n}{\partial t} = \left(1 + \frac{T_e}{T_i} \right) D_{i\perp} \frac{1}{r} \frac{\partial}{\partial r} r \left[\frac{\partial n}{\partial r} - n \frac{\partial \ln N_1(r, 0)}{\partial r} \right]. \quad (55)$$

The steady-state solution of the above is

$$n(r, z, t) = N_1(r, 0) N_2(z, 0), \quad e\varphi(r, z, t) = T_e \ln N_2(z, 0) - T_i \ln N_1(r, 0); \quad (56)$$

where $N_2(z, t)$ is the number of particles in a layer perpendicular to H and bounded by the side walls. This solution is asymptotically dependent on the density profile at the end of the fast stage as a result of the short circuiting of eddy currents in the plasma. The characteristic time of this stage is $\sim \tau_{i\perp}$. Figure 15 shows a simple example of the fast stage. The rapid relaxation of a small deviation from the ambipolar profile [Eq.

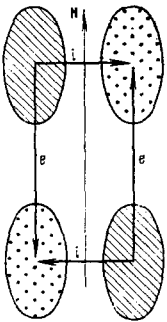


FIG. 15. Eddy currents during the rapid diffusion stage. Initial profile corresponds to the ambipolar profile $n(x, z, 0) = N_1(x)N_2(z)$ with condensations (cross hatched) and rarefactions (dots) of the plasma superposed on it.

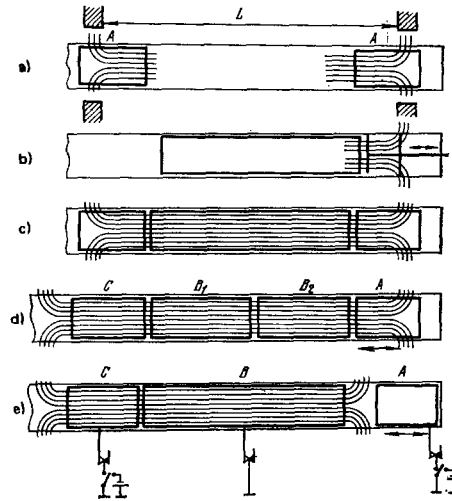


FIG. 16. Schematic diagram of experiments on plasma diffusion.⁵⁰ A, B, C—metallic cylinders. Thin lines—magnetic lines of force. Electrode A in apparatuses of Fig. 16 b and e is movable. Cylinder A could be replaced by a plane end electrode.

(56)] was considered in Ref. 53. Having determined the profile of Eq. (56), we can eliminate the potential from the initial system and obtain the usual equation of anisotropic diffusion with ambipolar coefficients along and across the magnetic field:

$$\frac{\partial n}{\partial t} = \left(1 + \frac{T_e}{T_i} \right) D_{i||} \frac{\partial^2 n}{\partial z^2} + \left(1 + \frac{T_i}{T_e} \right) \frac{D_{e\perp}}{r} \frac{\partial}{\partial r} r \frac{\partial n}{\partial r}. \quad (57)$$

It describes the evolution of the plasma profile with slow times. For the fundamental diffusion mode, for example, we have

$$n(r, z, t) = A \cos\left(\frac{z}{\Lambda_{||}}\right) J_0\left(\frac{r}{\Lambda_{\perp}}\right) e^{-t/\tau}, \quad (58)$$

$$\Lambda_{||} = L/\pi, \quad \Lambda_{\perp} = \frac{R}{2.405},$$

$$\frac{1}{\tau} = \frac{1}{\tau_{e||}} + \frac{1}{\tau_{a\perp}} = \quad (59)$$

$$+ \left(1 + \frac{T_i}{T_e} \right) \frac{D_{e\perp}}{\Lambda_{\perp}^2} + \left(1 + \frac{T_e}{T_i} \right) \frac{D_{i||}}{\Lambda_{||}^2}.$$

In the case of a long ($\tau_{e||} \gg \tau_{i\perp}$) apparatus the rapid diffusion stage, which leads to the ambipolar profile [Eq. (56)], occurs during a time $\sim \tau_{e||}$.

The long-standing efforts to determine experimentally the ambipolar diffusion regime have been encumbered by the fact that at $\rho_e \rho_i < \lambda_e \lambda_i$, where the magnetic field begins to have a substantial effect on the transverse ambipolar diffusion, plasma in dielectric apparatuses becomes unstable. The plasma lifetime in this case is considerably shorter than the classical value of Eq. (59). An unambiguous proof of achievement of the classical ambipolar diffusion regime was obtained experimentally in a decaying plasma.⁵⁰ Both quiescent and turbulent isothermal plasmas were obtained in apparatuses with conducting lateral walls (Fig. 16).⁴⁾ Both states were characterized by a definite margin of stability. The plasma could be transferred from one state into another at any given time by means of a con-

⁴⁾The majority of experiments described below were carried out in a decaying plasma and, therefore, all experimental curves correspond to $T_e = T_i = 300$ K.

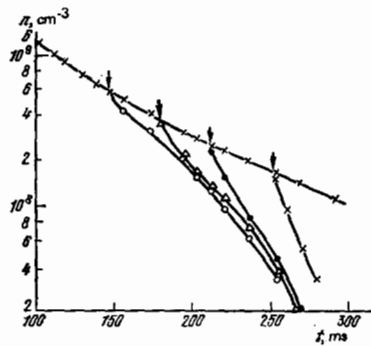


FIG. 17. Drop in plasma density along the axis of the apparatus for disconnected end and side electrodes. Arrows indicate transitions to a turbulent state when a pulsed voltage is applied to the probe.

trolled external effect. The transition from a quiescent state into a turbulent one is indicated by arrows in Fig. 17. In the first regime, the lifetime was determined by the classical transport coefficients. Figure 18 shows D_{a1} calculated from measured lifetimes, according to the equation $D_{a1} = \Lambda_1^2 (\tau^{-1} - D_{a1}/\Lambda_1^2)$; the longitudinal coefficient of ambipolar diffusion is assumed to be classical. Good agreement between calculations and experiment is evident. The presence of conducting walls (the end wall in the different variants of the experiment was both conducting and dielectric)⁵⁰ should lead to a change in the electric field in the plasma compared to Eq. (56) (see below in subsection c). Thus, for example, at $\tau_{e11} > \tau_{i1}$ and in the case of a mean free path lateral layer, there should be no longitudinal electric field for the fundamental diffusion mode [Eq. (58)]. Therefore, the multiplier $1 + (T_e/T_i)$ should be omitted from the second term in Eq. (59). The corresponding corrections to Eq. (59) under the experimental conditions of Ref. 50 do not exceed a factor of 2. Since the real plasma density profile could differ slightly from Eq. (58), allowance for these corrections would, evidently, exceed accuracy.

In recent years, a number of articles appeared (see, for example, Refs. 107–112), in which theoretical investigations were made of the anomalous diffusion resulting from random electric fields of large-scale

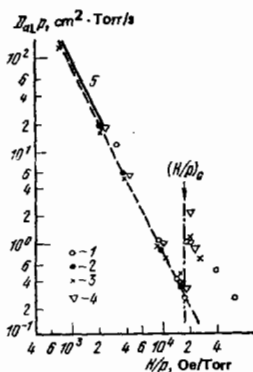


FIG. 18. Dependence of transverse ambipolar diffusion coefficient in a helium plasma on the magnetic field. Dashed line corresponds to classical theory. $R=2$ cm, $L=75-80$ cm. Pressure (Torr) = 5×10^{-2} (1), 9×10^{-2} (2), 0.3 (3) and 0.16 (4); 5—data of Ref. 70. Sharp increase at $H > H_w$ is due to occurrence of an instability.

thermodynamic equilibrium fluctuations (convection cells). It was asserted in these papers that at $\omega_{pe} \lesssim \Omega_e$ the basic contribution to particle transport should derive from this mechanism. The experimental data^{111,112} were in qualitative agreement with such a model. The foregoing experiments⁵⁰ were carried out over a broad range of densities up to $n \sim 10^7$ cm⁻³, at which value the ratio $\omega_{pe}/\Omega_e \lesssim 10^{-2}$ and the effect of equilibrium fluctuations, in accordance with Refs. 107–110 should be appreciable. However, noticeable deviations from the classical transport coefficients were not observed in a quiescent plasma. This agrees with the most consistent calculations,^{113–115} which show that thermal fluctuations should lead to only comparatively small corrections to the classical values.

As the plasma in a metallic chamber became unstable, there was an increase in the transverse diffusion of the plasma, which was practically identical to the case of a dielectric apparatus. The major cause of instability under the experimental conditions was violation of quasineutrality in the small-scale drift-type oscillations.^{51,116} Therefore, in a plasma of sufficiently high density for which the Debye radius is small, oscillations occurred only near the wall and the transverse diffusion in practically the entire apparatus was near-classical. At a low density, however, transverse diffusion increased considerably. Figures 19 and 20 show the experimental results. Clearly, calculated values of the coefficient of ambipolar diffusion across H at high density were close to experimental ones. The result was practically independent of the tube radius and of the kind and pressure of gas since the diffusion was basically determined by the electron-ion collisions. As the density decreased, the unstable plasma layer at the wall expanded and, eventually, filled the entire volume of the apparatus. The coefficient of transverse diffusion calculated from the lifetime was, moreover, approaching the value of Bohm's diffusion coefficient ($D_1 \sim D_B = cT/16eH$).⁷⁹

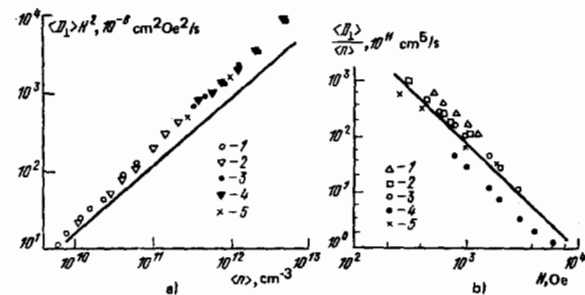


FIG. 19. a. Dependence of $\langle D_{a1} \rangle$ on the plasma density averaged over the cross section: 1, 2—data of Ref. 41, 3, 4, 5—data of Refs. 118, 119, H (kOe) = 0.5 (1, 3), 1.0 (2, 4), 3.0 (5). b. Dependence of transverse ambipolar diffusion coefficient (averaged over the cross section; diffusion is due to electron-ion collisions) on the magnetic field.^{50,117,118} (1—He, $\langle n \rangle = 3 \times 10^{11} - 3 \times 10^{12}$ cm⁻³, $R=4$ cm; 2—He, $\langle n \rangle = 2 \times 10^{10} - 10^{11}$ cm⁻³, $R=0.8$ cm; 3—He, $\langle n \rangle = 3 \times 10^{11} - 3 \times 10^{12}$ cm⁻³, $R=0.5$ cm; 4—He, $\langle n \rangle = 3 \times 10^{11} - 3 \times 10^{12}$ cm⁻³, $R=0.25$ cm; 5—Ar, $\langle n \rangle = 2 \times 10^{10} - 10^{11}$ cm⁻³, $R=0.8$ cm; straight line corresponds to the classical values of D_{a1} ; $\langle n \rangle$ —density averaged over the cross section).

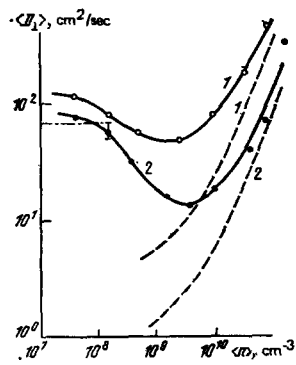


FIG. 20. Dependence of $\langle D_{a\parallel} \rangle$ on $\langle n \rangle$ in a dielectric apparatus.^{41,46} $R=2$ cm, $L=80$ cm, $p=3 \times 10^{-2}$ Torr, gas—He. Curve 1— $H=1$ kOe, 2— $H=2$ kOe. Dashed lines—classical diffusion coefficient; dash-dot lines—Bohm's diffusion coefficient.

Diffusion along the magnetic field was close to classical under all conditions. Figure 21 shows the values of the longitudinal diffusion coefficient which were determined from the measured values of the diffusion plasma lifetime in apparatus of variable length:

$$D_{a\parallel} = \Lambda_{\parallel} [\tau^{-1}(\Lambda_{\parallel}) - \tau^{-1}(\Lambda_{\parallel} \rightarrow \infty)]. \quad (60)$$

The effect of electric field distortion, due to the conducting walls, as compared to the ambipolar case, could be substantial only at $\tau_{e\parallel} \sim \tau_{i\perp}$; however, even in this case, the correction to Eq. (60) did not exceed a factor of 2 under the experimental conditions.

If the side walls of a chamber are inclined to the magnetic field at an angle α , according to Eqs. (25) and (46) diffusion even in a one-dimensional apparatus with dielectric walls is not ambipolar and occurs much faster. A qualitative picture of the flow of the electron and ion currents in this case is shown in Fig. 22a. Clearly, $\Gamma_{e\parallel, \perp} \neq \Gamma_{i\parallel, \perp}$ holds at not a single point in the apparatus and wall neutrality is achieved by the arrival of electrons and ions from different regions of the plasma. This effect was discovered and explained by Ganichev⁴⁶ and Zhilinskii.⁵² The decay constant for a one-dimensional profile $n = n_0 \cos(\xi/\Lambda_{\parallel})e^{-t/\tau}$ according to Eq. (46) is

$$\tau^{-1} = \frac{D(\tilde{\mu}^2)}{\Lambda_{\parallel}^2}. \quad (61)$$

The experimental results are in satisfactory agreement with theory (see Fig. 22b). The diffusion picture in an apparatus of limited length was more complex.⁵² In particular, the plasma lifetimes at different seg-

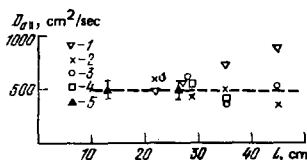


FIG. 21. Coefficient of longitudinal ambipolar diffusion in helium.^{41,46,50} 1— $R=0.8$ cm, $p=8 \times 10^{-2}$ Torr, $H=1$ kOe; 3— $R=0.8$ cm, $p=5 \times 10^{-2}$ Torr, $H=2.4$ kOe; 4— $R=0.5$ cm, $p=0.1$ Torr, $H=2$ kOe; 5— $R=0.5$ cm, $p=0.1$ Torr, $H=4$ kOe. Dashed line—classical value $D_{a\parallel} = 2D_{i\parallel}$.

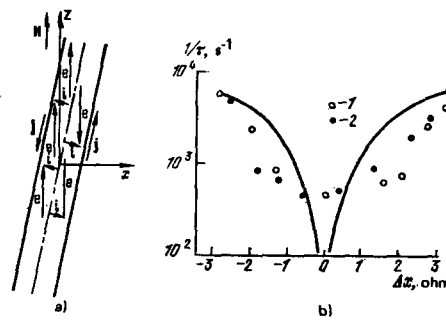


FIG. 22. a. Particle flows during diffusion in a dielectric apparatus with the axis inclined to the magnetic field. b. Effect of dielectric tube misalignment on the plasma lifetime.⁵² Experiments in He in a tube of length $L=90$ cm and radius $R=0.8$ cm, $H=1$ kOe, $p=0.1$ Torr. Angle between the tube axis and magnetic field $\alpha = \Delta x/L$ (1, 2—tube misalignment in two mutually perpendicular directions). Solid line—calculations by Eq. (61) for an infinitely long apparatus. Λ_{\parallel} assumed to be $R/2.4$.

ments of the length of the apparatus should be unequal. During a later stage, the decay should be again slowed down, a fact which was observed experimentally.

c. Diffusion in an apparatus with conducting walls

In this case, the short-circuiting effect takes place (Section 3). In a short ($\tau_{e\parallel} \ll \tau_{i\perp}$) apparatus a rapid removal of electrons along H to the ends charges the walls negatively. If the space charge layer, adjacent to the end wall, is collisionless, the potential at a point in the plasma with respect to the end is according to Eq. (50)

$$\varphi(r, z, t) = -\frac{T_e}{e} \ln \frac{4\Gamma_{e\parallel}^s(r, t)}{nv_e}, \quad (62)$$

where $\Gamma_{e\parallel}^s(r, t)$ is the electron current density at an end. The potential over almost the entire volume of the apparatus (except for small regions adjacent to the side wall) is determined by Eq. (62), and we also have

$$\left| \frac{\partial N_1(r, t)}{\partial t} \right| = 2\Gamma_{e\parallel}^s(r, t).$$

Therefore,

$$\varphi = -\frac{T_e}{e} \ln \frac{2|\partial N_1/\partial t|}{nv_e}, \quad (63)$$

and the density equation is

$$\frac{\partial n}{\partial t} = \frac{1}{r} \frac{\partial}{\partial r} D_{i\perp} r \left[\left(1 + \frac{T_e}{T_i} \right) \frac{\partial n}{\partial r} - \frac{T_e}{T_i} n \frac{\partial^2 N_1}{\partial r \partial t} \left(\frac{\partial N_1}{\partial t} \right)^{-1} \right]. \quad (64)$$

The above equation has a particular solution

$$n(r, z, t) = A J_0 \left(\frac{r}{\Lambda_{\perp}} \right) f(z) e^{-t/\tau_{sc}}, \quad (65)$$

which corresponds to decay with a short-circuiting time of $\tau_{sc} \approx \tau_{i\perp}$ ($\approx \tau_{e\parallel}$ in a long apparatus). The potential drop between a point in the plasma and the end electrode is determined by the motion of electrons along H , i.e. by the ratio of the rate of removal to an end $\partial N_1(r, t)/\partial t$ to the density at a given point $n(r, z, t)$ according to Eq. (63). For the profile in Eq. (65) the dependence of these values on r is the same for all values, so that the potential in the plasma is independent of r and there is no transverse (with respect to the magnetic field) electric field. In the case of a diffusion end layer the presence

of a transverse field results in the value of decay time being equal to $\tau_{i1} [1 + (T_e/3T_i)]^{-1}$. In all cases the potential in the plasma volume is "bound" to the end electrode and the transverse electric field is determined by the rate of removal of electrons along H. The situation changes only at distances of the order of $\Lambda_{||} \nu_e / \Omega_e$ from the side wall where the electron motion may no longer be considered as one-dimensional.⁷⁶ In a long apparatus ($\tau_{e||} \gg \tau_{i1}$), the electric field along H is determined by a layer adjacent to the side wall. The qualitative considerations of Refs. 5, 41 yield a value of the decay time in a short apparatus equal to $\tau_{i1} [1 + (T_e/T_i)]^{-1}$; the difference is especially significant in a nonisothermal plasma at $T_e \gg T_i$.

The nature of diffusion, determined by Eq. (64), strongly depends on the shape of the density profile. If in a short apparatus against the background of a profile with characteristic scales determined by the apparatus dimensions $\Lambda_{||}$ and Λ_{\perp} , there exist small-scale perturbations $\bar{\Lambda}_{||}$ and $\bar{\Lambda}_{\perp}$ (with the corresponding times $\bar{\tau}_{e||}$ and $\bar{\tau}_{e\perp}$), the effect of boundaries on the relaxation of harmonics with $\bar{\tau}_{i1} < \tau_{e||}$ is insignificant; they, generally speaking, spread in the same manner as in an infinite plasma. The evolution of inhomogeneities with $\bar{\tau}_{i1} > \tau_{e||}$ leads (as also in a dielectric apparatus) to establishment of a profile of the form $N_1(r)N_2(z)$ during a time $\sim \bar{\tau}_{i1}$. Subsequently, regardless of the fact that the density profile remains broken up on a scale $\bar{\Lambda}_{\perp}$, diffusion is determined by the size of the apparatus and proceeds with a large characteristic time $\tau_{i1} > \bar{\tau}_{i1}$.⁷⁶ The reason for this is that, with an accuracy of up to the slow transverse electron diffusion, $N_1(r, t) = \int_0^L n(r, z, t) dz$ can only decrease as a result of removal of electrons toward the ends. And in the case of a profile of the form $N_1(r)N_2(z)$, the densities in two adjacent columns, which are parallel to H and separated by $\bar{\Lambda}_{\perp}$, would tend to become the same during a time $\sim \bar{\tau}_{i1}$ only if the density in one of the columns is increasing.

Experiments on the diffusion of a quasistationary plasma in closed metallic apparatuses were the subject of several articles.^{79, 121-125} Moreover, a hot plasma pinch existed only at the central part of the chamber, while the remaining volume was filled with plasma as a result of diffusion from the near-axial regions. The electron temperature was much lower at the periphery than at the center. The main electron flow to the metallic wall had to proceed along H from the near-axial region and to produce a large negative potential drop between the chamber and the plasma, which almost entirely locks the electrons in at the periphery. The spatial density distribution in this case must be determined by ion diffusion. These considerations (by Zharinov) were confirmed experimentally.^{122, 123} Thus, possibility of non-ambipolar diffusion of electrons and ions in a magnetic field was shown in this work for the first time. However, it only indirectly testifies concerning the possibility of short circuiting the entire plasma volume. An attempt was made to discover this effect in a quasistationary system with the plasma uniformly filling the entire chamber cross section.¹²⁶ The results were essentially unsuccessful. The reason for this can apparently be attributed to the incorrect method used for mea-

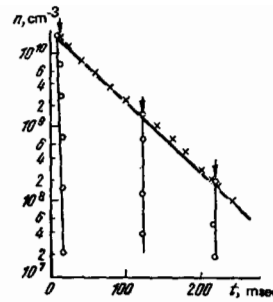


FIG. 23. Decay of helium plasma in a metallic chamber.¹²⁸ $R=2$ cm, $p=0.1$ Torr, $H=2$ kOe. End electrode simulated by a cylinder in a weak field. Arrow indicates instant when the end and side electrodes are connected.

asuring the diffusion coefficient.

Decaying plasma was the object of investigation in the second group of papers.^{41, 44-46, 70, 127} Direct measurements were used for the first time to show the effect of short circuiting on the lifetime of the entire plasma as a whole.⁴¹ However, the experimentally observed diffusion rate was considerably lower than predicted by the theory. In a number of subsequent papers contradictory data were obtained. Acceleration of diffusion decay in a metallic chamber was noted by Geissler.^{45, 70} The short-circuiting effect was not recorded at all in Ref. 44.

A detailed experimental investigation of the short-circuiting effect was carried out successfully only after the stabilizing effect of the side walls on the instability of the decaying plasma was discovered,⁵⁰ and the limits of the range of parameters for which the plasma remains quiescent were established. In these experiments the conducting cylindrical side surface was adjusted along the magnetic field and the end electrodes consisted of flat plates which were perpendicular or inclined to H, or were simulated by cylinder segments, coaxial with the side cylinder, and situated in the region of magnetic field (see Fig. 16). Both end electrodes (or one of them) could be connected electrically to the side cylinder at any instant during decay. Before the connection was made ambipolar decay described above was achieved and, subsequently, the short-circuiting regime. The nature of decay in both regimes was close to exponential (Fig. 23); however, the diffusion rate sharply increased (the lifetime decreased by more than two

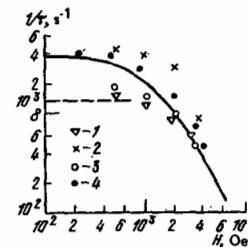


FIG. 24. Time of diffusion decay of a plasma in the case of short circuiting.¹²⁹ Helium, $R=1.9$ cm, $L=65$ cm, $p=0.1$ Torr. Solid curve— τ_{i1}^{-1} , dashed curve— $\tau_{e||}^{-1}$. Symbols: 1—3— one-sided short circuiting, 1—with plane end, 2—with cylindrical end in a weak field region, 3—with cylindrical end and compensation; 4—two-sided short circuiting with plane and cylindrical ends and compensation.

orders). Figure 24 shows the observed values of the plasma lifetime. In the case of short-circuiting on two sides under the experimental conditions we have $\tau_{\text{ell}} > \tau_{\text{il}}$ for the fundamental diffusion mode and, therefore, the lifetime should be close to τ_{il} (curve in Fig. 24). For a magnetic field $H < 1.5$ kOe and one-sided short-circuiting we have $\tau_{\text{ell}} \approx (2L/\pi)^2/D_{\text{el}} > \tau_{\text{il}}$. Consequently, in this case the lifetime in weak fields should be $\approx \tau_{\text{ell}}$ and as the field intensifies, it approaches τ_{il} . Both the nature of dependence on the magnetic field and the lifetime values agree with calculations; discrepancies are apparently due to the density profile differing from fundamental diffusion mode [Eq. (58)]. It is also possible that the potential applied in making a correction between the end and side electrodes in order to compensate an unknown contact potential difference, did alter somewhat the electric field in the plasma.

Since, in the case of short-circuiting, electrons escape mainly toward the end electrode and ions toward the side electrode, recording the current which flows between the two electrodes provides a mean for measuring the diffusion rate and plasma density. A comparison of data obtained by means of this method with the results of UHF resonator measurements is shown in Fig. 25.

d. Diffusion in the case of more complex boundary conditions

We shall consider several simple examples. If the potential difference between the end and side electrodes Φ_w in the aforementioned system (see Fig. 16 b and c) is changed, plasma decay in a short apparatus ($\tau_{\text{eH}} \gg \tau_{\text{il}}$) is described, as before, by Eqs. (63) and (64). The potential drop between the central plasma region and the wall in the case of short circuiting with the profile [Eq. (65)] and a collisionless layer is, according to Eq. (63)

$$e\varphi(z) = -T_e \ln \frac{2 \int_0^L f(z) dz}{\tau_{\text{il}} \bar{v}_e f(z)} \sim T_e \ln \frac{\tau_{\text{il}} \bar{v}_e}{L} \quad (66)$$

The electric field (orthogonal to the magnetic field) is absent from the main portion of the plasma volume and the potential drop [Eq. (66)] is confined to a thin layer of thickness of the order of $\delta = L \Gamma_{\text{el}}/\Gamma_{\text{eH}}$ at the side wall, in which transverse electron motion is substan-

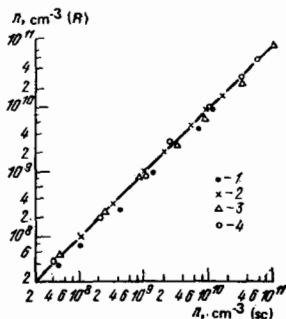


FIG. 25. Particle density obtained by the resonator method— $n(R)$ and by the short circuiting method— $n(SC)$, in a helium plasma in a tube with $R = 1$ cm, $p = 0.1$ Torr.¹³⁰ H (kOe)—0.2 (1), 0.45 (2), 1.0 (3) and 1.8 (4).

tial. If a potential Φ_w , which is negative with respect to the end, is applied to the side wall the situation hardly changes, the potential, as before, is "bound" to the end by Eq. (66) and an additional drop of the potential Φ_w will be confined to a layer of thickness $\sim \delta$ at the side wall. For positive values of $\Phi_w \approx \Phi_{w1}^0 = T_e / e \ln(\tau_{\text{il}} \bar{v}_e / L)$, the potential difference between the center and side wall becomes trivial. A further growth of Φ_w leads to a blocking of the transverse motion of ions and an electric field which is transverse to H is generated. According to subsection a, the transverse flow of ions will be considerably weaker than the diffusion flow if the potential drop in the plasma across H is $> \Phi_{w2}^0 = (T_i/e) \ln[R/\min(\rho_i, \lambda_i)]$, i.e., when

$$\Phi_w > \Phi_w^0 = (\Phi_{w1}^0 + \Phi_{w2}^0). \quad (67)$$

Starting from these values the diffusion decay time will increase with increasing Φ_w . Under these conditions (as also in a dielectric apparatus) a fast diffusion stage can be identified, which is not accompanied by particle escape to the walls and, as a result of eddy currents passing through the plasma, leads to establishment of the profile of Eq. (65). In order to evaluate the characteristic time for a slow stage τ , we shall assume that the electric field in this case blocks the motion of ions across H and of electrons along H . The rate of electron escape to the end electrode is proportional to $\tau_i^{-1} \exp[-e(\Phi_{w1} - \Phi_{w1}^0)/T_i]$ and of ion escape to the side wall is proportional to $\tau_i^{-1} \exp[-e(\Phi_{w2} - \Phi_{w2}^0)/T_i]$, where Φ_{w1} is the potential drop between the plasma center and the end, and Φ_{w2} , between the side wall and the center. Since these rates should be equal and $\Phi_w = \Phi_{w1} + \Phi_{w2}$, the plasma lifetime is

$$\tau \approx \tau_{\text{il}} \exp\left(\frac{e\Phi_w - e\Phi_w^0}{T_e + T_i}\right). \quad (68)$$

At times exceeding τ , the plasma decays exponentially $\sim \exp(-t/\tau)$. According to Eq. (63), the radial electric field should be nonexistent at this stage. Since the motion of ions across H is also blocked (occurring during $\tau \ll \tau_{\text{il}}$), $E_r = 0$ in the main plasma volume for the same reason. The evolution, therefore, is determined solely by the diffusion currents, and $\Gamma_{\text{eH}} \ll D_{\text{eH}} n_0 / \Lambda_{\text{H}}$ and $\Gamma_{\text{il}} \ll D_{\text{il}} n_0 / \Lambda_{\text{L}}$, i.e., the density in the main plasma volume is almost constant; small additions, dependent on the coordinates, preserve the passage of Γ_{eH} and Γ_{il} flows. The exponential growth of $\tau(\Phi_w)$ in the "negative end" regime continues until τ becomes equal to τ_{il} . At that instant the slow process—longitudinal ion diffusion, not taken into account in derivation of Eq. (68)—begins to operate and the plasma motion along H becomes ambipolar.

In a long apparatus ($\tau_{\text{eH}} \gg \tau_{\text{il}}$), the potential is "bound" to the side wall, so that at $\Phi_w < \Phi_w^0$ the longitudinal electric field is nonexistent. By changing Φ_w , the diffusion lifetime may be increased to τ_{el} .

Figure 26 shows a comparison of the experimental values of $\tau(\Phi_w)$ with theoretical ones.⁷⁶ Curves 2 and 3 were calculated using Eq. (68), and for curve 1, a similar formula for a long apparatus was used. Since the contact potential difference was unknown, one experimental point was made to fall on the calculated curve.

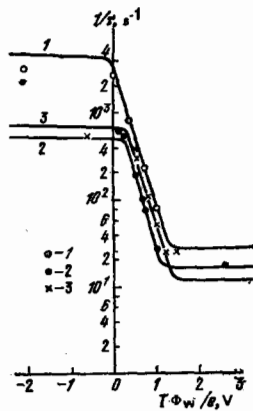


FIG. 26. Dependence of diffusion lifetime $\tau(\Phi_w)$ on Φ_w .⁷⁶ Experiment: helium in a tube with $R=1.9$ cm, $L=75$ cm; 1— $H=0.5$ kOe, $p=0.05$ Torr; 2— $H=2$ kOe, $p=0.05$ Torr; 3— $H=2$ kOe, $p=0.08$ Torr.

Differences occurring at large τ were the result of instabilities observed in this regime; differences at small τ were associated, possibly, with the fact that the density profile differed from the fundamental diffusion mode.

After the diffusion along H becomes ambipolar, the electron flow toward an end can not diminish further with increasing Φ_w . The continuing growth of Φ_w leads only to an exponential decrease of $\Gamma_{i\perp}$. The diffusion across the magnetic field at $\tau_{i\parallel} \sim \tau_{e\perp}$ may be even much slower than ambipolar. Figure 27 shows an example of such a slow plasma decay.

The use of various boundary conditions opens ways for controlling the local values of the plasma lifetime and density. Thus, for example, if only a portion of the side surface of a tube is conducting, short circuiting it by an end leads to a rapid escape of the plasma from only this portion of the volume. Figure 28 shows the time-dependent density of a decaying plasma inside a small conducting cylinder of length L_B when the latter is short circuited by an end electrode (see Fig. 16d). In the fast stage we have $\tau \approx \tau_{i\perp}$ (long apparatus); a slow decrease in the density in the final stage corresponds to ambipolar diffusion along H from the main plasma into the volume of the cylinder L_B .

Since under the gas-discharge conditions the plasma

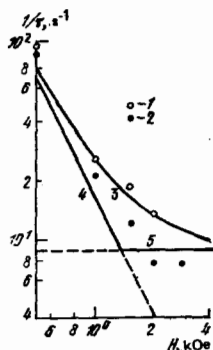


FIG. 27. Decay time in the negative end regime in He.⁷⁵ $R=1.9$ cm, $L=70$ cm, $p=0.12$ Torr. 1—ends under a floating potential (ambipolar regime); 2—negative ends ($\Phi_w=2.5$ V). Calculated curves: 3— τ_{a1}^{-1} , 4— τ_{a1}^{-1} , 5— τ_{a1}^{-1} .

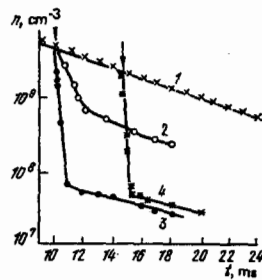


FIG. 28. Plasma decay in a small cylinder in He. $R=1$ cm, $L=80$ cm, $L_B=5$ cm, $p=0.1$ Torr, $H=1.8$ kOe; 1—without short circuiting; 2— $\Phi_w=0$; 3 and 4— $\Phi_w=-15$ V. Arrows indicate the instant of short circuiting.

density is self-consistently coupled to the electric field and the electron temperature, the use of the short-circuiting effect provides an opportunity to control the local plasma parameters (see, for example, Ref. 132).

The presence of emitting electrodes should lead to a large number of interesting phenomena. We shall consider, for example, diffusion in a short apparatus with a dielectric side wall and a thermal emitter as an end electrode.

Since an effective emitter can generate practically any electron flow along H , a region of width of the order of $\delta = LD_{e\perp}/D_{e\parallel}$ adjoining the side wall may function as a conducting boundary. The electron flow in that region is directed basically across the magnetic field and the transverse diffusion is almost ambipolar. However, in the main volume of the plasma $r \approx R - \delta$ the short-circuiting effect is achieved, ions escape across H and electrons escape onto the emitter (Fig. 29a). The density drop between the central plasma and the boundary of the ambipolar diffusion region may be estimated as follows. The transverse ion and electron flows are $\Gamma_{i\perp} \sim (n_0 - n_1)D_{i\perp}/R$ and $\Gamma_{e\perp} \sim n_1D_{e\perp}/\delta$, respectively. If we equate the two, we obtain

$$\frac{n_0}{n_1} - 1 \sim \frac{L}{R} \frac{\tau_{i\perp}}{\tau_{e\perp}} \gg 1. \quad (69)$$

Mixed diffusion of this type was actually observed experimentally under the conditions where a certain voltage φ was applied between the end electrodes.⁵³ It is evident from Fig. 29b that the diffusion rate in a dielectric apparatus with an emitting electrode may be close to values corresponding to short circuiting.

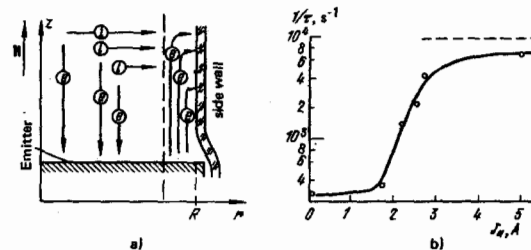


FIG. 29. Diffusion in the presence of an emitting electrode.⁵³ a. Diagram of eddy current flow in the plasma. b. Plasma decay time in a short apparatus as a function of the emitter heating current; $p=0.1$ Torr, $R=0.6$ cm, $L=30$ cm, $H=2.5$ kOe, $\varphi=10$ V. Dashed line—decay constant for the short circuiting regime ($\tau_{sc} = (R/2.4)^2/2D_{i\perp}$). Gas—helium.

e. Diffusion probe in a magnetic field

In the problems considered above, bounding surfaces enclosed the plasma on the outside. The opposite situation is frequently encountered, when a solid is placed in the plasma. As an example of this, we shall discuss the problem of an electrostatic diffusion probe in a weakly-ionized, quiescent plasma without an external current. The most widespread are cylindrical probes oriented along the magnetic field (a —radius, $2b$ —length). We shall consider only those aspects which bear directly on the problem of plasma diffusion. The diffusion motion of particles exerts a considerable influence on the voltage-current characteristic of a probe, if the layer thickness (r_s) or radius a is greater than the mean free path of the random migration of the particles. Therefore, in a magnetic field such effects are most significant for electrons. For the sake of simplicity, we shall assume $r_s \ll a$ and, instead of a cylindrical probe, we shall consider an ellipsoid of revolution with semi-axes a and b .

If a large positive potential is applied to a probe, electron saturation current will flow to it. The electric field in the plasma retards the ion motion, $e\varphi = -T_e \ln(n/n_0)$. The density profile $n^{(e)}(r)$ and the probe current are determined by the anisotropic diffusion equation

$$\frac{D_{e\perp}}{r} \frac{\partial}{\partial r} r \frac{\partial n^{(e)}}{\partial r} + D_{e\parallel} \frac{\partial^2 n^{(e)}}{\partial z^2} = 0 \quad (70)$$

with zero boundary condition at the probe surface, $n^{(e)}(\infty) = 1$. If

$$a\Omega_e \gg b\nu_e, \quad (71)$$

the value of the electron saturation current (Bohm's current) is^{80,81}

$$J_e^{(B)} = \frac{4n_0 e [1 + (T_i/T_e)] D_{e\perp} \sqrt{a^2 \Omega_e^2 - b^2 \nu_e^2}}{\nu_e \arctg \sqrt{a^2 \Omega_e^2 / b^2 \nu_e^2 - 1}} \quad (72)$$

(n_0 is the density of the unperturbed plasma) and is practically independent of b . The plasma density is perturbed in the volume of the electron ellipsoid with semi-axes $\sim a$ and $a\Omega_e/\nu_e$, which considerably exceeds the probe volume.

Experimental verification of Eq. (72) was undertaken in Refs. 82, 83, 133. The observed dependence of the electron saturation current on H was close to theoretical.^{83,133} Quantitative agreement with Eq. (72) was obtained.⁸² The thin foil probe had the shape of a square of side $2a' = 0.3$ mm, and was placed perpendicular to the magnetic field. The density of the decaying isothermal plasma was measured independently by means of an UHF resonator method and the short circuiting method (see above). In calculations, $a = 2a'/\sqrt{\pi}$ was used. Figures 30 and 31 show that for a broad range of plasma densities and magnetic fields the experimental and theoretical values of the electron saturation current in various gases in apparatuses with dielectric and conducting walls agree fairly well. The dependence of the probe current on time, upon changing from electron to ion saturation current is also well described by the diffusion theory.¹³⁴

It should be especially noted that the probe current

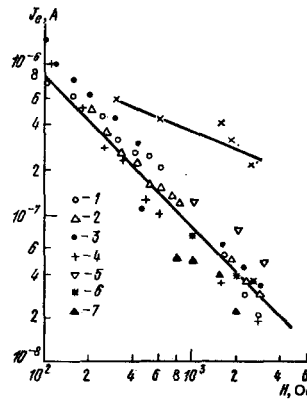


FIG. 30. Dependence of electron saturation current on the magnetic field at $n = 8 \times 10^{18} \text{ cm}^{-3}$. Lower curve—calculated by Eq. (72) with the classical values of $D_{e\perp}$, upper curve—with anomalous values determined from the plasma lifetime in the apparatus. Symbols 1–4—experiments in Ar in an apparatus with dielectric walls, $R = 1.2$ cm, $L = 80$ cm, p (Torr) = 0.02 (1), 0.06 (2), 0.1 (3) and 0.4 (4); 5—He, $R = 1.2$ cm, $L = 35$ cm, $p = 0.3$ Torr; 6 and 7—He, apparatus with conducting walls, $R = 2$ cm, $L = 75$ cm, 6— $p = 0.1$ Torr, 7— $p = 0.16$ Torr.

in the experiments was determined by the classical transport coefficients both in the stable and turbulent plasmas in which the transverse diffusion time, on the scale of the entire apparatus, decreased in comparison with the classical value by more than an order of magnitude (see curves 1 and 2 in Fig. 30). On the other hand, values of the electron saturation current substantially exceeding that of Bohm, were observed in a number of studies carried out in a gas-discharge plasma with $T_e \gg T_i$.^{79,83,122} This is possibly due to the plasma generation in the near-probe region (see also Ref. 136).

We shall now calculate the dependence of the electron and ion currents J_e and J_i on the probe potential φ_p . In particular, we shall determine to which point on the volt-ampere characteristic does the space potential φ_s correspond. We shall assume the space charge layer to be collisionless and the motion of both electrons and ions to the probe to be governed by diffusion (other cases are considered in Ref. 87). The ion saturation current when $\gamma = b \sqrt{1 + (\Omega_i^2/\nu_i^2)}/a > 1$, for example, is^{80,81}

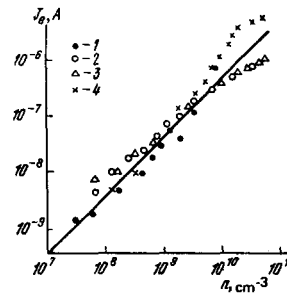


FIG. 31. Dependence of electron saturation current to a probe on the plasma density in Ar. Dielectric apparatus, $R = 1.2$ cm, $L = 80$ cm, $H = 2.4$ kOe. Solid line—calculated by Eq. (72) with the classical values of $D_{e\perp} \cdot p$ (Torr) = 0.01 (1), 0.06 (2), 0.1 (3) and 0.4 (4).

$$J_i^{(B)} = \frac{8\pi en_0 [1 + (T_e/T_i)] D_{i\parallel} \sqrt{\gamma^2 - 1}}{\sqrt{1 + (\Omega_i^2/\nu_i^2)} \ln [(\gamma + \sqrt{1 - \gamma^2})/(\gamma - \sqrt{1 - \gamma^2})]} \quad (73)$$

In this situation, the field in the plasma retards the electrons: $e\varphi = T_e \ln(n/n_0)$. The corresponding density profile $n^{(i)}$ is determined by an equation similar to Eq. (70). The plasma is perturbed in an ellipsoid of semi-axes b and $b\sqrt{1 + (\Omega_i^2/\nu_i^2)}$. We shall turn our attention to the following circumstance, common to a majority of problems which we have considered. At large values of φ_p , electrons and ions flow onto the probe, which satisfies the condition in Eq. (71), from various regions of space (Fig. 32). This property should be preserved also at intermediate values of φ_p . We shall consider, for example, particle motion in the electron ellipsoid. In the absence of an electric field, practically all the electrons present in this ellipsoid, in the case of diffusion motion, will arrive on the absorbing surface of the probe. The motion of ions across H occurs much faster and long H, much slower than that of the electrons. Therefore, in the case of diffusion, ions from this ellipsoid can not reach the probe. An electric field will not change the situation, since the field E_z may not exceed $(T_e/e)\partial n/\partial z$ (otherwise a heavy flow of electrons from the probe would ensue). Thus, if the electron current to the probe is large (comprises a significant fraction of Bohm's current), it should be collected from the electron ellipsoid. But the potential profile in the latter should correspond to the Boltzmann ion distribution. The density in this region is described, as before, by the anisotropic diffusion equation. The solution of the latter is

$$n(r) = n_0 \left[1 - \frac{J_e}{J_e^{(B)}} (1 - n^{(e)}) \right]. \quad (74a)$$

However, in the ion ellipsoid the opposite situation occurs. The Boltzmann distribution is realized for electrons and

$$n(r) = n_0 \left[1 - \frac{J_i}{J_i^{(B)}} (1 - n^{(i)}) \right], \quad (74b)$$

Thus, in the case of a concurrent flow of ion and electron currents to the probe, the field is characterized by a quadrupole and the current is short circuited in the plasma. The profile of Eq. (74) may be violated only in

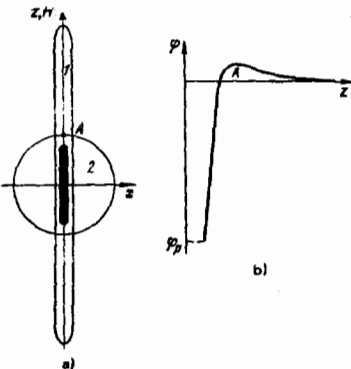


FIG. 32. a. Electron (1) and ion (2) ellipsoids in the case of particle motion by diffusion and $a\sqrt{1 + (\Omega_i^2/\nu_i^2)} < b < a\Omega_e/\nu_e$ (the probe is cross hatched); b. Potential profile along the z -axis for $J_e < J_e^{(B)}$ (point A corresponds to the boundary of the region where the electron and ion ellipsoids overlap).

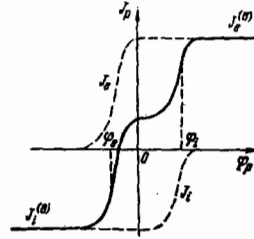


FIG. 33. Schematic view of the current-voltage characteristic of a diffusion probe for $J_e^{(B)} \sim J_i^{(B)}$. Potentials φ_e and φ_i correspond to the blocking of electron (ion) current; both are determined according to Eqs. (75) and (76), respectively, by the condition $J_{e,i}(\varphi_e = \varphi_{e,i}) = J_{e,i}^{(B)}/e$.

a small region near the probe (where the ellipsoids overlap), where the electrons and ions may escape onto the probe along and across H, respectively. According to Eq. (74a), the plasma density $n(A)$ at the electron ellipsoid boundary in the overlap region is $[1 - (J_e/J_e^{(B)})]n_0$. Since the condition $n|_w = 0$ must be satisfied on the probe surface, the drop in density in the overlap region is relatively large and the electric field should retard the electrons. The electron flow in it is preserved and they move in one dimension along H. The potential profile in the case of motion along the z -axis toward the probe is shown schematically in Fig. 32b.⁵ The potential drop in the electron ellipsoid is $-(T_e/e) \ln[1 - (J_e/J_e^{(B)})]$ and in the overlap region [according to Eq. (50)], it is $(T_e/e) \ln[4\Gamma_{e,i}/n(A)\nu_e]$. Thus, the electron branch of the characteristic is described by the following expression:

$$\varphi_p = -\frac{T_e}{e} \ln \left(1 - \frac{J_e}{J_e^{(B)}} \right) - \frac{T_e}{e} \ln \{ \pi en_0 a^2 \tilde{\nu}_e (J_e^{-1} - J_e^{(B)-1}) \}. \quad (75)$$

The value of probe potential φ_e , at which J_e constitutes a significant fraction (1/e) of the saturation current, is (at $T_i \lesssim T_e$) negative and of large absolute value; if $\varphi_p > \varphi_e$, the electron current is close to Bohm's. The ion branch of the characteristic may be obtained similarly to Eq. (75). For example, at $\Omega_i > \nu_i$, $a\Omega_i/\Omega_i < b\nu_i$, using Eq. (50a) we obtain

$$\varphi_p = \frac{T_e}{e} \ln \left(1 - \frac{J_i}{J_i^{(B)}} \right) + \frac{T_i}{e} \ln \{ 4\pi en_0 a b \tilde{\nu}_i (J_i^{-1} - J_i^{(B)-1}) \}. \quad (76)$$

In order to block the ion current, a considerable positive potential φ_i (at $T_e \sim T_i$) must be applied to the probe. Equations (75) and (76) describe the total voltage-current characteristic. Its shape is quite complex, as is evident from the plot in Fig. 33. The distinguishing feature of this characteristic is the presence of a plateau—essentially both saturation currents flow onto the probe over a certain range of values of φ_p . The width of the plateau for the above case is

$$\varphi_i - \varphi_e = \frac{T_i}{e} \ln \frac{22en_0 a b \tilde{\nu}_i}{J_i^{(B)}} - \frac{T_e}{e} \ln \frac{5.5en_0 a^2 \tilde{\nu}_e}{J_e^{(B)}} + \frac{(T_e + T_i) \ln 0.64}{e}. \quad (77)$$

The most distinct plateau should be seen at $J_e^{(B)} \sim J_i^{(B)}$. Such a curve contains much useful information concerning the plasma parameters and provides a means to determine these by a variety of independent meth-

⁵A similar nonmonotonic potential profile was obtained by Sanmartin for the case of a probe in a fully-ionized plasma.¹³⁵

ods.⁸⁷ The existing experimental data which confirm the above considerations are discussed in Refs. 137 and 138. We shall simply note that the well-defined plateaux, as far as we know, have not been observed experimentally. The reason for this is apparently that under the experimental conditions the width of the plateaux, as estimates show, is comparatively small, and $J_e^{(B)} \gg J_i^{(B)}$.

We have assumed above that the partial temperatures were unperturbed by the probe current takeoff. Meanwhile, energy transfer between electrons and the heavy plasma component is difficult. Therefore, electron current takeoff may be accompanied by a considerable distortion of the electron distribution function in the near-probe region. The conditions under which these effects must be taken into account are considered in other articles.^{104,137}

- ¹V. L. Granovskii, *Elektricheskiĭ tok v gaze* (Electric Currents in Gases), v. 2, Nauka, M., 1971.
- ²V. E. Golant, A. N. Zhilinskiĭ, and I. E. Sakharov, *Osnovy Fiziki plazmy* (Fundamentals of Plasma Physics), Atomizdat, M., 1977.
- ³M. Mitchner and C. Kruger, *Partially Ionized Gases* (Russ. Transl., Mir, M. 1976) (wiley 1973).
- ⁴M. D. Gabovich, *Fizika i tekhnika plazmennyykh istochnikov ionov* (Physics and Technology of Plasma Ion Sources), Atomizdat, M., 1972.
- ⁵V. E. Golant, *Usp. Fiz. Nauk* **79**, 377 (1963) [*Sov. Phys. Usp.* **5**, 161 (1963)]; in: VIII ICIPG, Vienna, 1967, p. 447.
- ⁶F. Boeschoten, *Plasma Phys.* **6**, 339 (1964).
- ⁷V. I. Stafeev and É. I. Karakushan, *Magnitodiody* (Magnetic Diodes), Nauka, M., 1975.
- ⁸G. Weiss, *Fizika gal'vanomagnitnykh poluprovodnikovyykh privorov i ikh primeniya* (Physics of Galvanomagnetic Semiconductor Instruments and Applications), Energiya, M., 1974.
- ⁹H. Suhl and W. Shockley, *Phys. Rev.* **75**, 1617 (1949); *ibid.* **76**, 180 (1949).
- ¹⁰R. Rosa, *Magnetohydrodynamic Energy Conversion* (Russ. Transl. Mir, M., 1970) (McGraw, 1968).
- ¹¹B. N. Gershman, *Dinamika ionosfernoi plazmy* (Dynamics of the Ionospheric Plasma), Nauka, M., 1974.
- ¹²J. Ratcliff, *Introduction to Physics of the Ionosphere and Magnetosphere* (Russ. Transl., Mir, M., 1975).
- ¹³Z. Bauer, *Physics of Planetary Ionospheres* (Russ. Transl. Mir, M., 1976) (Springer-Verlag, 1973).
- ¹⁴B. B. Kadomtsev, V: *Voprosy teorii plazmy* (in: Problems of Plasma Theory), Atomizdat, M., 1964, No. 4, p. 188.
- ¹⁵A. A. Galeev and R. Z. Sagdeev, *ibid.*, No. 7, p. 3.
- ¹⁶B. B. Kadomtsev, *Kollektivnye yavleniya v plazme* (Collective Phenomena in Plasma), Nauka, M., 1976.
- ¹⁷V. N. Tsytoich, *Teoriya turbulentnoi plazmy* (Theory of a Turbulent Plasma), Atomizdat, M., 1971.
- ¹⁸A. A. Vedenov, *Teoriya turbulentnoi plazmy* (Theory of a Turbulent Plasma), VINITI, M., 1965.
- ¹⁹V. P. Dokuchaev, *Izv. Akad. Nauk SSSR, Ser. geofiz.* **5**, 783 (1959) [*Izv. Acad. Sci. USSR, Geophys. Ser.*].
- ²⁰A. V. Gurevich and E. E. Tsedilina, *Usp. Fiz. Nauk* **91**, 609 (1967) [*Sov. Phys. Usp.* **10**, 214 (1967)].
- ²¹I. Shkarovskii, T. Johnstone, and M. Bachinskiĭ, *Kinetika chastits plazmy* (Kinetics of Plasma Particles), Atomizdat, M., 1969.
- ²²V. L. Ginzburg and A. V. Gurevich, *Usp. Fiz. Nauk* **70**, 201 (1960) [*Sov. Phys. Usp.* **2**, 115 (1960)].
- ²³V. L. Ginzburg, *Rasprostraneniye elektromagnitnykh voln v plazme* (Propagation of Electromagnetic Waves in a Plasma), Nauka, M., 1967.
- ²⁴V. A. Bailey, *Phil. Mag.* **9**, 360 (1930).
- ²⁵R. Y. Bickerton, *Proc. Phys. Soc., Ser. B* **70**, 305 (1957).
- ²⁶V. E. Golant, A. P. Zhilinskiĭ, and M. V. Terent'eva, see Rev. 5.
- ²⁷L. L. Pasechnik and V. V. Yagola, *Zh. Tekh. Fiz.* **40**, 108 (1970) [*Sov. Phys. Tech. Phys.* **15**, 74 (1970)]; *Ukr. Fiz. Zh.* **13**, 1564 (1968).
- ²⁸M. A. Biondi, *Phys. Rev.* **93**, 1136 (1954).
- ²⁹A. P. Zhilinskiĭ, I. F. Liventseva, and L. D. Tsendin, *Zh. Tekh. Fiz.* **47**, 304 (1977) [*Sov. Phys. Tech. Phys.* **22**, 177 (1977)].
- ³⁰F. G. Baksht, I. L. Korobova, and B. Ya. Moizhes, *Zh. Tekh. Fiz.* **40**, 843 (1970) [*Sov. Phys. Tech. Phys.* **15**, 653 (1970)].
- ³¹W. Schottky, *Phys. Zs.* **25**, 329 (1924).
- ³²M. A. Biondi and S. C. Brown, *Phys. Rev.* **75**, 1700 (1949).
- ³³I. S. Townsend, *Phil. Mag.* **25**, 429 (1938).
- ³⁴V. S. Golubev and V. L. Granovskii, *Radiotekh. Elektron.* **7**, 663 (1962) [*Radio Eng. Electron Phys. (USSR)*].
- ³⁵L. W. Holway, *J. Geophys. Res.* **70**, 3635 (1965); *Phys. Fluids* **8**, 1207 (1965).
- ³⁶V. N. Gershman, *Radiotekh. Elektron.* **1**, 720 (1956) [*Radio Eng. Electron Phys. (USSR)*].
- ³⁷V. P. Dokuchaev, *Izv. Vyssh. Uchebn. Zaved., Radiofiz.* **3**, 50 (1960) [*Sov. Radiophys.*].
- ³⁸W. P. Allis, in: *Handbuch der Physik*, v. 21, Springer-Verlag, B., 1956.
- ³⁹A. V. Gurevich, *Zh. Eksp. Teor. Fiz.* **44**, 1302 (1963) [*Sov. Phys. JETP* **17**, 878 (1963)].
- ⁴⁰A. Simon, *Phys. Rev.* **98**, 317 (1955).
- ⁴¹V. E. Golant and A. P. Zhilinskiĭ, *Zh. Tekh. Fiz.* **32**, 127 (1962); **32**, 1313 (1962) [*Sov. Phys. Tech. Phys.* **7**, 84 (1962); **7**, 970 (1963)].
- ⁴²I. B. Chekmarev, *ibid.* **42**, 253 (1972) [*ibid.* **17**, 203 (1972)].
- ⁴³I. B. Chekmarev, *Izv. Akad. Nauk SSSR, Ser. Mekhanika zhidkosti i gaza*, No. 1, 92 (1977) [*Izv. Acad. Sci. USSR, Ser. Mechanics of Fluids and Gas*].
- ⁴⁴S. Takeda, K. Minami, and T. Uno, *Phys. Rev. Lett.* **18**, 829 (1967).
- ⁴⁵K. H. Geissler, *Phys. Fluids* **13**, 935 (1970).
- ⁴⁶A. A. Ganichev, V. E. Golant, A. P. Zhilinskiĭ, *et al.*, *Zh. Tekh. Fiz.* **34**, 77 (1964) [*Sov. Phys. Tech. Phys.* **9**, 58 (1964)].
- ⁴⁷N. D. Angelo, in: *Physics of High-Temperature Plasma* (Russ. Transl., Mir, M., 1972, p. 214).
- ⁴⁸R. W. Motley, *Q-machines*, Acad. Press, N. Y., 1975.
- ⁴⁹N. S. Buchel'nikova, in: VIII ICIPG, Vienna, 1967, p. 433.
- ⁵⁰A. P. Zhilinskiĭ and B. V. Kuteev, *Zh. Tekh. Fiz.* **45**, 255 (1975); **45**, 2092 (1975) [*Sov. Phys. Tech. Phys.* **20**, 163 (1975); **20**, 1316 (1975)].
- ⁵¹V. V. Bulanin and A. P. Zhilinskiĭ, *ibid.* **41**, 1374 (1972); **41**, 2469 (1972) [*ibid.* **16**, 1081 (1972); **16**, 1960 (1972)].
- ⁵²A. P. Zhilinskiĭ and A. S. Smirnov, *ibid.* **47**, 2079 (1977) [*ibid.* **22**, 1208 (1977)].
- ⁵³A. P. Zhilinskiĭ and B. V. Kuteev, *ibid.* **48**, 2047 (1978) [*ibid.* **23**, 1168 (1978)].
- ⁵⁴A. V. Gurevich and E. E. Tsedilina, *Geomag. aëronom.* **5**, 251 (1965); *ibid.* **6**, 255 (1966).
- ⁵⁵E. E. Tsedilina, *ibid.* **5**, 679 (1965).
- ⁵⁶V. A. Rozhanskiĭ and L. D. Tsendin, *Fiz. Plazmy* **1**, 904 (1975) [*Sov. J. Plasma Phys.* **1**, 494 (1975)]; *Zh. Tekh. Fiz.* **47**, 2017 (1977) [*Sov. Phys. Tech. Phys.* **22**, 1173 (1977)].
- ⁵⁷V. A. Rozhanskiĭ and L. D. Tsendin, *Fiz. Plazmy* **3**, 382 (1977) [*Sov. J. Plasma Phys.* **3**, 217 (1977)].
- ⁵⁸S. P. Voskoboĭnikov, *et al.*, *ibid.* **6**, 730 (1980) [*ibid.* **6**, (in press) (1980)].
- ⁵⁹G. G. Novikov, S. F. Tsygankov, and L. N. Rubtsov, *Izv. Vyssh. Uchebn. Zaved., Radiofiz.* **19**, 171 (1975) [*Sov. Radio-Phys.*].
- ⁶⁰K. H. Lloyd and G. H. Haerendel, *J. Geophys. Res.* **78**, 7389 (1973).

- ⁶¹G. Haerendel and M. Scholer, *Space Research VII*, North Holland, Amsterdam, 1974.
- ⁶²M. Giles and G. Martelli, *Planet and Space Sci.* 15, 357 (1967); M. Giles, *J. Plasma Phys.* 10, 317 (1973).
- ⁶³A. Simon, *J. Geophys. Res.* 75, 6287 (1970).
- ⁶⁴N. J. Zabusky, J. H. Doles, and F. W. Perkins, *ibid.* 78, 711 (1973).
- ⁶⁵S. R. Goldman, S. L. Ossakow, D. L. Book, *et al.*, *ibid.* 79, 1471 (1974).
- ⁶⁶A. J. Scannapicco, S. L. Ossakow, D. L. Book, *et al.*, *ibid.* 80, 2879 (1975).
- ⁶⁷D. L. Book, S. L. Ossakow, and S. R. Goldman *ibid.* 79, 2913 (1974).
- ⁶⁸J. H. Doles, N. J. Zabusky, and F. W. Perkins, *ibid.* 81, 5987 (1976).
- ⁶⁹I. B. Chekmarov, T. Yu. Simkina, and V. S. Yuferev, *Plasma Phys.* 19, 15 (1976).
- ⁷⁰K. H. Geissler, *Phys. Rev.* 171, 179 (1968); *Plasma Phys.* 10, 127 (1970).
- ⁷¹D. R. Whitehouse and H. B. Wollman, *Phys. Fluids* 6, 1470 (1963).
- ⁷²R. L. Monroe, *Can. J. Phys.* 51, 564 (1973); *ibid.* 52, 94 (1974).
- ⁷³A. A. Gurin, *Fiz. Plazmy* 2, 422 (1976) [*Sov. J. Plasma Phys.* 2, 230 (1976)].
- ⁷⁴L. Tonks, *Phys. Fluids* 3, 758 (1960).
- ⁷⁵A. P. Zhilinskiĭ and B. V. Kuteev, *Pis'ma Zh. Tekh. Fiz.* 2, 412 (1976) [*Sov. Tech. Phys. Lett.* 2, 160 (1976)].
- ⁷⁶A. P. Zhilinskiĭ, V. A. Rozhanskiĭ, and L. D. Tsendin, *Fiz. plazmy* 4, 586 (1978) [*Sov. J. Plasma Phys.* 4, 326 (1978)].
- ⁷⁷V. A. Rozhanskiĭ and L. D. Tsendin, *ibid.* 4, 388 (1978) [*ibid.* 4, 218 (1978)]; V. A. Rozhanskiĭ, in: XIV ICIPG, Grenoble, 1979, p. C7-515.
- ⁷⁸F. G. Baksht, G. A. Dyuzhev, B. I. Tsirkel', *et al.*, *Zh. Tekh. Fiz.* 47, 1630 (1977) [*Sov. Phys. Tech. Phys.* 22, 944 (1977)].
- ⁷⁹D. Bohm, in: *The Characteristics of Electrical Discharges in Magnetic Fields*, Eds. A. Guthrie and R. Wakerling, N. Y., 1949, Ch. I-IV.
- ⁸⁰I. M. Cohen, *Phys. Fluids* 12, 2536 (1969).
- ⁸¹I. M. Cohen, *AIAA Journ.* 5, 63 (1967).
- ⁸²A. P. Zhilinskiĭ, B. V. Kuteev, N. V. Sakharov, *et al.*, *Fiz. plazmy* 3, 1028 (1972) [*Sov. J. Plasma Phys.* 3, 568 (1972)].
- ⁸³F. G. Baksht, G. A. Dyuzhev, B. I. Tsirkel', *et al.*, *Zh. Tekh. Fiz.* 47, 2269 (1977) [*Sov. Phys. Tech. Phys.* 22, 1313 (1977)]; preprint FTI AN SSSR, No. 533, Leningrad, 1977.
- ⁸⁴M. Sato, *Phys. Fluids* 15, 2427 (1972).
- ⁸⁵M. Sugawara, *ibid.* 9, 797 (1966).
- ⁸⁶K. Nyogi and I. M. Cohen, *ibid.* 16, 69 (1973).
- ⁸⁷V. A. Rozhanskiĭ and L. D. Tsendin, *Zh. Tekh. Fiz.* 48, 1647 (1978) [*Sov. Phys. Tech. Phys.* 23, 932 (1978)].
- ⁸⁸L. Huxley and R. Crompton, *Diffusion and Drift of Electrons in Gases* (Russ. Transl., Mir, M., 1977) (Wiley Interscience, 1974).
- ⁸⁹M. Scholer and H. Haerendel, *Planet. and Space Sci.* 19, 915 (1971).
- ⁹⁰M. Lampert and P. Mark, *Current Injection in Solids* (Russ. Transl., Mir, M., 1973) (Acad. Pr., 1970).
- ⁹¹V. L. Bonch-Bruевич and S. G. Kalashnikov, *Fizika poluprovodnikov* (Physics of Semiconductors), Nauka, M., 1972.
- ⁹²T. R. Kaiser, W. M. Pickering, and C. D. Watkins, *Planet. and Space Sci.* 17, 519 (1969).
- ⁹³V. A. Rozhanskiĭ and L. D. Tsendin, *Geomag. aéron.* 17, 1002 (1977).
- ⁹⁴V. S. Anoshkin, A. P. Zhilinskiĭ, G. G. Petrov, *et al.*, *ibid.* 19, 1058 (1979); preprint FTI AN SSSR, No. 600, Leningrad, 1979.
- ⁹⁵A. P. Zhilinskiĭ, *et al.*, v: II Vsesoyuznoe soveshchanie po neodnorod. ionosfere (in: II All-Union Conference on Inhomog. Ionosphere), Ashkhabad, 1979.
- ⁹⁶A. J. Baxter, *Planet. and Space Sci.* 23, 973 (1975).
- ⁹⁷H. Foppl, G. Haerendel, L. Haser, *et al.*, *J. Geophys. Res.* 73, 21 (1968); G. Haerendel and R. Lust, in: *Particles and Fields in the Magnetosphere*, Reidel, Dordrecht, 1970.
- ⁹⁸M. Wescott, J. D. Stolarik, and J. P. Heppner, *J. Geophys. Res.* 74, 3469 (1969).
- ⁹⁹I. Langmuir, *Phys. Rev.* 28, 727 (1929).
- ¹⁰⁰V. L. Granovskiĭ, *Dok. Akad. Nauk SSSR* 23, 880 (1939).
- ¹⁰¹Termoemissionnye preobrazovateli i nizkotemperaturnaya plazma (Thermoemission Converters and Low-Temperature Plasma), Eds. B. Ya. Moizhes and G. E. Pikus, Nuaka, M., 1973.
- ¹⁰²F. G. Baksht and V. R. Yur'ev, *Zh. Tekh. Fiz.* 49, 905 (1979) [*Sov. Phys. Tech. Phys.* 24, 535 (1979)].
- ¹⁰³I. I. Litvinov, *Zh. Prikl. Mat. Teor. Fiz.*, No. 1, 52 (1977).
- ¹⁰⁴F. G. Baksht, *Zh. Tekh. Fiz.* 48, 1782 (1978) [*Sov. Phys. Tech. Phys.* 23, 1014 (1978)].
- ¹⁰⁵C. H. Su and S. H. Lam, *Phys. Fluids* 6, 1479 (1963).
- ¹⁰⁶I. M. Cohen, *ibid.* 6, 1492 (1963); *ibid.* 8, 2097 (1965).
- ¹⁰⁷J. B. Taylor and B. McNamara, *ibid.* 14, 1492 (1971).
- ¹⁰⁸G. Vahala, *ibid.* 16, 1876 (1973).
- ¹⁰⁹H. Okuda, J. M. Dawson, and W. M. Hooke, *Phys. Rev. Lett.* 29, 1658 (1972).
- ¹¹⁰H. Okuda, *Phys. Fluids* 17, 375 (1974).
- ¹¹¹M. N. Gurnee, W. M. Hooke *et al.*, *Phys. Rev. Ser. A* 5, 158 (1972).
- ¹¹²T. Tamana, R. Prater, and T. Ohkawa, *Phys. Rev. Lett.* 30, 431 (1973).
- ¹¹³S. Ishimaru and M. N. Rosenbluth, *Phys. Fluids* 13, 2778 (1970).
- ¹¹⁴S. Ishimaru and T. Tange, *J. Phys. Soc. Japan* 36, 603 (1974).
- ¹¹⁵S. Ishimaru, *Basic Principles of Plasma Physics* (Russ. Transl., Atomizdat, M., 1975) (Benjamin-Cummings, 1973).
- ¹¹⁶A. P. Zhilinskiĭ, *Zh. Tekh. Fiz.* 42, 925 (1972) [*Sov. Phys. Tech. Phys.* 17, 734 (1972)].
- ¹¹⁷A. I. Anisimov, N. I. Vinogradov, V. E. Golant, *et al.*, *ibid.* 34, 89 (1964) [*ibid.* 9, 68 (1964)].
- ¹¹⁸A. I. Anisimov, N. I. Vinogradov, V. E. Golant, *et al.*, *ibid.* 33, 1370 (1963) [*ibid.* 8, 1020 (1964)].
- ¹¹⁹A. I. Anisimov, V. N. Budnikov, N. I. Vinogradov, *et al.*, *Nucl. Fusion Suppl.*, part III, 1230 (1962).
- ¹²⁰A. I. Anisimov, N. I. Vinogradov, *et al.*, *Zh. Tekh. Fiz.* 32, 1197 (1962) [*Sov. Phys. Tech. Phys.* 7, 884 (1963)].
- ¹²¹A. Simon, Report No. 366, II Geneva Conference on Peaceful Uses of Atomic Energy, 1958.
- ¹²²A. V. Zharinov, *At. Energ.* 7, 215 (1959); *ibid.* 10, 368 (1961).
- ¹²³L. I. Elizarov and A. V. Zharinov, *Yad. sintez* (Nucl. Fusion), suppl., part II, 699 (1962).
- ¹²⁴M. A. Vlasov, *Pis'ma Zh. Eksp. Teor. Fiz.* 2, 274 (1965); 2, 297 (1965) [*JETP Lett.* 2, 174 (1965); 2, 189 (1965)]; *Zh. Eksp. Teor. Fiz.* 51, 715 (1966) [*Sov. Phys. JETP* 24, 475 (1967)].
- ¹²⁵F. Schwirzke, *Zs. Naturforsch.* 18a, 889 (1963); *Phys. Fluids* 9, 2244 and 2250 (1966); *ibid.* 10, 183 (1967).
- ¹²⁶L. L. Pasechnik, V. G. Naumovets, and A. S. Popvich, *At. Energ.* 31, 275 (1971) [*Sov. J. At. Energy*].
- ¹²⁷I. A. Vasil'eva, V. L. Granovskiĭ, and A. F. Chernovolenko, *Radiotekh. Elektron.* 5, 1516 (1960) [*Radio Eng. Electron. Phys.* (USSR)].
- ¹²⁸A. P. Zhilinskiĭ and B. V. Kuteev, *Zh. Tekh. Fiz.* 45, 2083 (1975) [*Sov. Phys. Tech. Phys.* 20, 1311 (1975)].
- ¹²⁹A. P. Zhilinskiĭ, B. V. Kuteev, and A. S. Smirnov, *ibid.* 48, 707 (1978) [*ibid.* 23, 416 (1978)].
- ¹³⁰A. P. Zhilinskiĭ and B. V. Kuteev, *ibid.* 48, 610 (1978) [*ibid.* 23, 358 (1978)].
- ¹³¹A. P. Zhilinskiĭ and B. V. Kuteev, *Pis'ma Zh. Tekh. Fiz.* 2, 412 (1976) [*Sov. Tech. Phys. Lett.* 2, 160 (1976)].
- ¹³²A. A. Ivanov, *et al.*, *Fiz. plazmy* 5, 1029 (1979) [*Sov. J. Plasma Phys.* 5, 576 (1979)].
- ¹³³T. Dote and H. Amemiya, *Japan J. Appl. Phys.* 3, 789 (1964).

¹³⁴V. M. Voronov, A. P. Zhilinskiĭ, B. V. Kuteev, *et al.*, *Fiz. plazmy* **3**, 1037 (1977) [*Sov. J. Plasma Phys.* **3**, 573 (1977)].

¹³⁵J. Sanmartin, *Phys. Fluids* **13**, 103 (1970).

¹³⁶A. P. Zhilinskiĭ, B. V. Kuteev, V. A. Rozhanskiĭ, *et al.*, v: *Trudy II Vsesoyuznoĭ shkoly po diagnostike plazmy* (in: *Proceedings of the II All-Union School on Plasma Diagnostics*), Tashkent, 1979.

¹³⁷B. V. Kuteev and V. A. Rozhanskiĭ, *Pis'ma Zh. Tekh. Fiz.* **4**, 118 (1978) [*Sov. Tech. Phys. Lett.* **4**, 49 (1978)].

¹³⁸B. V. Kuteev, V. A. Rozhanskiĭ, and L. D. Tsengin, *Beitrage Plasmaphys.* **19**, 123 (1979).

Translated by Yu. Ksander